Exercise-Induced Engagement of the IL-15/IL15Rα axis Promotes Anti-Tumor Immunity

Dafna Bar-Sagi (Dafna.Bar-Sagi@nyumc.org)
New York University School of Medicine https://orcid.org/0000-0003-2597-8948
Emma Kurz
New York University School of Medicine
Tanner Dalton
Columbia University Irving Medical Center
Sorin Shadaloey
New York University School of Medicine
Emily Vucic
New York University School of Medicine
Rafael Winograd
New York University Langone Health
Carolina Hirsch
New York University School of Medicine

Article

Keywords: Tumor Infiltration, Aerobic Exercise, Murine Models, Pancreatic Cancer, Epinephrine, PD-1 Blockade

Posted Date: January 18th, 2021

DOI: https://doi.org/10.21203/rs.3.rs-130050/v1

Exercise-Induced Engagement of the IL-15/IL15Rα axis Promotes Anti-Tumor Immunity

Authors: Emma Kurz[1^], Carolina Alcantara Hirsch[1,3], Tanner Dalton[2], Sorin Alberto Shadoloey[1], Emily Vucic[3], Rafael Winograd[4], **Dafna Bar-Sagi**[3*]

Affiliations:

[1]Department of Cell Biology, NYU Grossman School of Medicine, 550 1st Avenue, New York, NY, 10016

[2]Department of Cell Biology, Columbia University Irving Medical Center, 630 W 168th St. New York, NY, 10032

[3]Department of Biochemistry and Molecular Pharmacology, NYU Grossman School of Medicine, 550 1st Avenue, New York, NY, 10016

[4]Permultter Cancer Center, NYU Langone Health, 160 East 34th Street, New York, NY, 10016

(*) symbol indicates corresponding author information. (^) indicates first authorship.

Corresponding author contact: dafna.bar-sagi@nyulangone.org

One Sentence Summary: Exercise induces tumor protection and anti-tumor immunity in PDA.

Abstract

Tumor-infiltrating immune cells play a central role in controlling cancer development and progression, as well as in responses to therapeutic interventions. However, the mechanisms that control their mobilization, composition, and function are not completely understood. Here, we show that aerobic exercise is sufficient to induce an intra-tumoral expansion of activated CD8 T cells and a reduction in tumor growth in murine models of pancreatic cancer. Specifically, exercise-induced spikes in epinephrine promote a systemic immune mobilization and accumulation of tumor-infiltrating IL15Rα+ CD8 T cells. This sub-population of activated CD8 T cells is responsible for the tumor protective and immune activating benefits of aerobic exercise, as both are abrogated in the context of IL-15 antagonism. Notably, the anti-tumor effect of aerobic exercise is potentiated by PD-1 blockade, suggesting a therapeutically exploitable link between an exercise-oncology axis and immune intervention strategies in a largely intractable disease.

MAIN TEXT

A growing body of evidence indicates that frequent structured exercise is associated with decreased incidence of cancer and cancer-associated mortalities[1,2,3,4,5]. Preclinical studies utilizing murine models of breast cancer, liver cancer, and melanoma have implicated modulation of tumor vascularity, sex/growth hormone signaling, metabolic alterations, and immune cell engagement as potential mechanisms underlying the tumor-protective effects of exercise[6,7,8,9]. Despite these advances, little is known about the anti-tumor effects of exercise in the context of pancreatic ductal adenocarcinoma (PDA), a deadly disease for which current therapeutic options are woefully limited. In the present study we sought to identify local and systemic factors that could precipitate exercise-dependent tumor protective effects in pancreatic cancer.

Routine aerobic exercise restricts pancreatic tumor growth

To assess the impact of aerobic exercise on pancreatic tumor growth, we subjected animals to a mild intensity forced treadmill-running exercise regimen [5x/week; 30 mins; 15 cm/sec][10,11], hereafter referred to as aerobic exercise **(Schematic Figure 1a)**. In a slow-progressing autochthonous genetic model of PDA [p48-Cre;LSL-KRas^{G12D} / KC mice], aerobic exercise led to a pronounced delay in disease development, as evidenced by preservation of the acinar compartment and an associated reduction in desmoplastic reaction and metaplastic conversion **(Figure 1b, Extended Data 1a)**. We next examined the effect of aerobic exercise on tumor growth in an orthotopic model of PDA, wherein wild-type (WT) mice are subjected to intra-pancreatic injection of p53$^{R172H/+}$-KRAS^{G12D} (KPC) mutant cells and are sacrificed 3–4 weeks post-operation (post-op)[12]. In this model, aerobic exercise resulted in a reduction in tumor weight when initiated on post-op Day 1 concurrent with tumor implantation (**Figure 1c, Extended Data 1b**), or on post-op Day 12, when mice bear already-established tumors (**Figure 1d).** Notably, prolonging the duration (time) or increasing the intensity (speed) of aerobic exercise did not result in an additional degree of tumor protection in the KPC orthotopic model (**Extended Data 1c**). In aggregate, these findings indicate that aerobic exercise provides tumor protective benefits in the setting of both pancreatic tumor initiation and disease progression.

Exercise-mediated tumor protection requires CD8 T cells

Aerobic exercise has been known to modulate immune function and immune cell mobilization[13, 14]. The potential relevance of these modulatory effects to exercise-induced tumor protection is suggested by the loss of protection in athymic nude (**Figure 2a**) or Rag1KO mice (**Extended Data 2a**). As these results indicate an essential role for mature lymphocytes, we performed an unbiased analysis of the intra-tumoral immune milieu using single cell RNA sequencing (sc-RNA seq). Comparison of leukocytes isolated from exercise and control orthotopic KPC tumors revealed an approximate five-fold expansion of CD8 T cells (Cluster 1) in the tumors of exercised mice (**Figure 2b, 2g**). This increase in the number of CD8 T cells was corroborated using multiplex immune-fluorescence microscopy (**Figure 2c**). Subsequent analysis of the gene expression profile of the expanded CD8 T cell (Cluster 1) population demonstrated a distinctively activated and cytotoxic phenotype, evidenced by high expression of *Gzmk, Gzmb, Icos, CD28,* and *Ccl5* (**Extended Data 2b**). Upstream canonical pathway analysis also showed a significant upregulation of a cytotoxic/anti-tumor program in this population (**Figure 2d**). Using flow cytometry, we confirmed that intra-tumoral CD8 T cells isolated from exercised animals bear a distinctive cytotoxic and activated phenotype as compared to control animals (**Figure 2e, Gating Strategy Extended Data 2c**). Based on these observations, we hypothesized that this population is essential for exercise-mediated reduction in tumor growth in PDA. To test this hypothesis, CD8 T cells were depleted in control and exercised mice by the serial administration of a targeted depleting antibody (**Extended Data 2d**). In the absence of CD8 T cells, no reduction in tumor growth was observed in exercised mice (**Figure 2f**), indicating the essentiality of CD8 T cell expansion and activation in exercise-induced tumor protection.

In addition to activated CD8 T cells (Cluster 1), the most prevalent immune populations detected in both exercise and control tumors on sc-RNA seq included exhausted CD8 T cells (Cluster 2), myeloid suppressor cells (Cluster 3), CD4 T cells (Cluster 4), NK cells (Cluster 5), and B cells (Cluster 6) (**Figure 2b).** With the exception of a notable decrease in the fraction of myeloid suppressor cells (Cluster 3), no change in the relative fraction of intra-tumoral immune cells that comprise these clusters was observed between exercise and control tumors (**Figure 2g**). The mechanisms underlying the exercise-dependent decrease in the abundance of myeloid suppressor cells remains to be determined. However, the contribution of this change to the anti-tumor effect

of exercise likely reflects a decrease in myeloid-derived immune tolerant signals upstream of effector T cells. This immunologic hierarchy has been previously reported in PDA[15,16,17] and is consistent with our data documenting the complete dependency of exercise-induced tumor protection on activated CD8 T cells (**Figure 2f**).

Exercise-induced increase of intra-tumoral CD8 T cells is dependent on peripheral lymphocyte mobilization

Aerobic exercise-induced leukocytosis (EIL) and subsequent redistribution is a phenomenon mediated, in part, through exercise-associated spikes in epinephrine (Epi) that mobilize various immune populations to peripheral blood[18,19,20]. The contribution of EIL to our observed exercise-induced intra-tumoral immune alterations is suggested by the doubling of serum Epi levels detected at 30 minutes post-exercise with concomitant fractional increases in peripheral and intra-tumoral T cells (**Figure 3a-b**). This conclusion is further supported by the finding that treatment of exercised mice with non-selective beta-adrenergic blocker propranolol showed a reversal of both tumor protection and CD8 T cell expansion and activation (**Figure 3c-d**). Based on these findings, we sought to determine whether the increase in peripheral blood lymphocytes is required for exercise-mediated intra-tumoral CD8 T cell expansion. To this end, we utilized Fingolimod (FTY720), a drug known to induce marked lymphopenia via inhibition of lymphocyte egress from thymus or secondary lymphoid organs (SLO)[21,22,23]. Consistent with its mode of action, FTY720 abrogated the increase in total T cells and CD8 T cells in the blood of exercised mice (**Extended Data 3a,c).** Of note, FTY720 treatment also reversed exercise-induced increases in intra-tumoral CD8 T cells and abrogated exercise-mediated tumor protection (**Figure 3e-f, Extended Data 3b**). These findings implicate both adrenergic-mediated-EIL and peripheral migration of T cells as essential facilitators of the tumor protective and immune-modulatory effects of exercise in this disease model.

IL15/IL15Rα axis is required for exercise-induced tumor protection

The role of IL-6, IL-8, and IL-15, cytokines that are upregulated during strenuous exercise, in mediating the metabolic and immune responses to tissue damage has been well established[24,25]. Of the above, only free IL-15 and secreted IL-15/IL15rα complexes (IL-15 bound to the alpha subunit of IL-15 receptor) have been shown to promote CD8 T cell survival and induce a cytotoxic

phenotype through signal transduction in a *cis* or *trans* manner, respectively[26,27,28]. As we consistently observed a cytotoxic CD8 T cell phenotype in the tumors of exercised mice, we set out to test whether IL-15 responsive cells may contribute to exercise-induced anti-tumor immunity. Using flow cytometry and multiplex immune-fluorescence microscopy, we observed a significant increase in the fraction and number of IL15Rα+ CD8 T cells in the tumors of exercised mice, with no change in IL15Rα+ CD4 T cells (**Figure 4a-b)**. Phenotypic analysis of the tumor-infiltrating IL15Rα+ subset of CD8 T cells in exercised mice showed a significant upregulation of proliferation and activation markers compared to their IL15Rα negative counterparts, consistent with engagement of IL-15R signaling (**Figure 4c**). The essentiality of this axis was further established by demonstrating that treatment of exercised mice with an IL-15 neutralizing antibody was sufficient to reverse both exercise-mediated tumor protection and intra-tumoral increase of activated IL15Rα+ CD8 T cells (**Figure 4d-f, Extended Data Figure 3d**). These data support a role for the IL-15/IL15Rα+ axis in exercise-mediated intra-tumoral immune activation.

We next addressed the question of whether IL-15Rα+ CD8 T cells, akin to their parent population, may undergo beta-adrenergic-dependent peripheral mobilization via EIL. To this end, mice were sacrificed 30 minutes after completion of exercise and the levels of IL-15Rα+ CD8 T cells in the periphery were assayed. Consistent with an EIL-based mobilization mechanism observed for exercise-induced increase in intra-tumoral activated CD8 T cells (**Fig 3d-e**), exercise induced an increase in the number of IL-15Rα+ CD8 T cells in peripheral blood (**Extended Data 3e**), and this effect was mimicked by the administration of a physiological dose of epinephrine, albeit on a smaller scale (**Figure 4g**). In addition, treatment of mice with the beta-blocker propranolol inhibited the exercise-induced increase of IL-15Rα+ CD8 T cells in the tumor, indicating adrenergic-mediated mobilization of this cell population (**Figure 4h).** Furthermore, based on an earlier study reporting IL-15 production in tumors[29], we performed an analysis of levels of IL-15 in KPC orthotopic tumors and found it is produced by both immune and non-immune cellular compartments (**Figure 4i**), suggesting the possibility that IL15Rα+ CD8 T cells may be engaged by their cognate cytokine in the PDA microenvironment. Collectively, these observations support a role for both systemic and localized engagement of the IL-15/IL-15Rα+ signaling axis in mediating exercise-induced anti-tumor immunity and protection.

Aerobic exercise synergizes with α-PD-1 therapy

Given our observations that intra-tumoral CD8 T cells, including IL-15Rα+ CD8 T cells display selectively high expression of the exhaustion marker PD-1 in exercised animals (**Figure 2e, Extended Data 4a**), we tested whether the immune-modulatory effects of exercise could be enhanced when combined with α-PD-1. Treatment of mice with a PD-1 blocking antibody over the course of aerobic exercise was accompanied by a global enhancement of exercise-dependent anti-tumor modulatory effects, evidenced by increases in the total number of CD3+ T cells (**Extended Data 4b**), CD8 T cells (**Figure 5a**), and the proliferative, activated, and cytotoxic phenotype of this latter population (**Figure 5b**). In addition, we observed an increase in the number of tumor-infiltrating IL-15Rα+ CD8 T cells in exercised mice treated with α-PD-1, suggesting that these cells may be responsive to checkpoint blockade (**Figure 5c, Extended Data 4c**). Importantly, combination of exercise and α-PD-1 led to a significantly more effective reduction in tumor growth compared to exercise alone (**Figure 5d**), suggesting that PD-1 blockade could enhance the tumor-protective and immune-activating efficacy of aerobic exercise in pancreatic cancer.

Discussion

Our findings uncover a hitherto unknown link between exercise-induced immune cell mobilization and pancreatic tumor protection involving IL-15 signaling and cytotoxic T cell-mediated anti-tumor immunity (**Figure 5e).** The consistency of the tumor-protective effects observed across multiple experimental murine models of pancreatic tumorigenesis suggests a broadly applicable association between aerobic exercise and tumor control in pancreatic cancer. Furthermore, the finding that even mild exercise is sufficient to profoundly alter the intra-tumoral immune milieu points to the potential utility and accessibility of physical-activity-based interventions for pancreatic cancer patients, a population with significant morbidities[30].

To date, the impact of aerobic exercise on immune cell redistribution and activation has been shown to be principally mediated by circulating serum cytokines or altered systemic metabolites that directly promote immune cell activation in the perpihery[6,9]. Our findings add a new dimension to the immune-modulatory effects of aerobic exercise by implicating the pancreatic tumor itself as a site of immune cell activation through the production of IL-15 by tumor and stromal cells.

Furthermore, the failure of exercise to induce protection in a syngeneic sub-Q model of PDA (**Extended Figure 1d**) suggests that a cross-talk between systemic EIL and an organ-specific tumor microenvironment may constitute an important determinant of the protective benefits of exercise.

In conclusion, our work demonstrates that exercise alone can prime the pancreatic tumor microenvironment for improved responsiveness to immune-based therapeautics. This insight should provide the basis for future combinatorial approaches involving aerobic exercise and immune-modulatory agents in treatment-resistant and immune-supressed solid tumors like pancreatic cancer.

STAR Methods:

Murine exercise, disease models, and in-vivo treatment regimens

C57BL/6, Rag1KO, and FoxNude athymic mice were purchased from Jackson Labs (Bar Harbor, ME) and bred in-house. LSL-KRAS$^{G12D/+}$; p48$^{Cre/+}$ (KC) mice were bred in the Division of Comparative Medicine mouse facility at New York University Langone Medical Center. Both male and female mice were used, as indicated, and animals were age matched within each experiment. For orthotopic studies, 8-10 week old mice were administered intra-pancreatic injections of 4662, 1203, or FC1242 KPC cells derived from LSL-KRAS$^{G12D/+}$ p53$^{R172H/+}$; p48$^{Cre/+}$ (KPC) mice, as previously described[31]. Briefly, cells were suspended in PBS with 50% Matrigel (BD Biosciences, Franklin Lakes, NJ) and either $5x10^4$ or $1x10^5$ KPC cells were injected into the pancreas via laparotomy. Mice were sacrificed on Day 21 for analyses, unless otherwise indicated. For subcutaneous studies, $1x10^6$ KPC cells were implanted into the flank of age-matched mice and mice were sacrificed at Day 33 or upon tumor ulceration. For all experiments, unless otherwise indicated, exercised mice were involuntarily placed on a Rodent 5-lane treadmill (Harvard Apparatus, Cat No: 76-0895), for 30 minutes per day at 15 cm/second, for a minimum of 5 days/week. In the 3 days leading up to sacrifice, exercise mice were obligately exercised, regardless of previous number of consecutive days exercised. Mice that were unable to complete treadmill running routine exercise were removed from the experiment. For initial experiments, sham control mice in matched experiments were placed on a stationary (0 cm/sec) treadmill for the same duration of time as experimental mice. After ten independent experimental repeats using

sham controls, experiments were performed with control mice remaining in their cage when no difference in sham control and control mice in the cage were observed. Where indicated, neutralizing antibodies directed against CD8 (200 μg, clone 2.43), IL-15 (200 μg, clone AIO.3), or PD-1 (200 μg, clone RMP1-14) were utilized (all from BioXcell, West Lebanon, NH) 3x weekly using regimens previously described[32,33,34]. Where indicated, mice were treated every day intraperitoneally (i.p.) with 2mg/kg with FTY720 (Sigma Aldrich). Stocks of FTY720 were resuspended in DMSO (20 mg/mL) and stored at -80ºC;. for injection, FTY720 was first resuspended in 2% βhydroxypropyl-cyclodextrin in PBS and diluted at 45% volume in PBS (Sigma Aldrich) based on previous protocols[35]. Where indicated, mice were provided either normal drinking water or .5g/L propranolol (Sigma Aldrich) drinking water and bifurcated into control and exercise cohorts[36]. All studies were approved by the Institutional Animal Care and Use Committee at NYU School of Medicine. Experiments were conducted in accordance with the NYU School of Medicine policies on the care, welfare, and treatment of laboratory animals. All experiments met or exceeded the standards of the Association for the Assessment and Accreditation of Laboratory Animal Care, International (AAALAC), the United States Department of Health and Human Services, and all local and federal animal welfare laws.

Cellular Preparation, Flow Cytometry, and FACS

Single cell suspensions of PDA tumors were prepared for flow cytometry as described previously with slight modifications[17]. Briefly, pancreata were placed in cold 2% FACS (cold PBS with 2% FBS) with Collagenase IV (1 mg/mL; Worthington Biochemical, Lakewood, NJ), Trypsin inhibitor (1mg/mL; EMD Millipore, Billerica, MA) and DNase I (2 U/mL; Promega, Madison, WI), and minced with scissors to sub-millimeter pieces. Tissues were then incubated at 37°C for 20 minutes with gentle shaking every 5 minutes and then passed through a 70μm mesh and centrifuged at 350g for 5 minutes. Cell pellets were re-suspended in FACS. After blocking FcγRIII/II with an anti-CD16/CD32 mAb (eBiosciences, San Diego, CA), cells were labeled by incubating $1x10^6$ cells with 1 μg of fluorescently conjugated mAbs directed against mouse CD44 (IM7), PD-1 (29F.1A12), CD3 (17A2), CD4 (RM4-5), CD8 (53-6.7), CD45 (30-F11), CD11b (M1/70), Gr1 (RB6-8C5), MHC II (M5/114.15.2), IFNγ (XMG1.2), ICOS (15F9), CD69 (H1.2F3), IL-15ralpha (6B4C88), Ki67 (16A8), CD140a (APA5), EPCAM (G8.8), CD34 (MEC14.7), (all BioLegend, San Diego, CA), IL-15 (Thermo Fisher, clone 34559), T-bet

(eBio4B10), and Granzyme B (NGZB). For flow cytometry of whole blood, PBMC were isolated by overlaying whole blood diluted 1:1 in PBS over an equal amount of Ficoll (GE Healthcare, Princeton, NJ). Cells were then spun at 2100 RPM and the buffy coat harvested as described[37]. Dead cells were excluded from analysis using zombie yellow (BioLegend). Flow cytometry was performed on the Attune NxT Flow Cytometer (ThermoFisher, Waltham, MA). FACS-sorting was performed on the SY3200 (Sony, Tokyo, Japan). Data were analyzed using FlowJo Version 10.6.1 (Treestar, Ashland, OR).

Histology, Immunofluorescence, and Microscopy

Tissues were fixed for 48 hours in 10% buffered formalin at 4°C and embedded into paraffin in a Leica Peloris automated processor. Five-micron sections of the paraffin-embedded tissues were stained with hematoxylin and eosin (H&E) or Gomori Trichrome, where appropriate. Histology was analyzed on a Zeiss LSM700 confocal microscope. The percentage of acinar area (fibrosis) in each slide was calculated on Adobe Photoshop software by dividing the number of pancreatic acinar pixels (or Trichrome Gomore blue stained pixels) over the total number of tissue pixels present in each field of view (FOV). Where appropriate, FFPE samples were stained with Akoya Biosciences® Opal™ multiplex automation kit (Akoya Biosciences, Menlo Park, CA). Automated staining was performed on Leica BondRX® autostainer (Leica Microsystems, Inc., Buffalo Grove, IL). The protocol was performed according to manufacturers' instructions. Primary antibodies included CD3 (Biorad, cat # MCA1477T), CD8 (Cell Signaling Tech, cat # 98941), IL15ra (ThermoFisher, cat # PA5-79467) and CK8 (TROMA-I) [TROMA-I, deposited to the DSHB by Brulet, P. / Kemler, R. (DSHB Hybridoma Product TROMA-I)]. Briefly, all slides underwent sequential epitope retrieval, antibody incubation and tyramide signal amplification (TSA). Primary and secondary antibodies were removed during epitope retrieval steps while fluorophores remain covalently attached to the epitope. Multispectral Image Acquisition and Analysis was performed on a Vectra® Polaris multispectral imaging system (Akoya Biosciences, Menlo Park, CA) and the fluorophores spectrally unmixed using either Phenochart (for whole slide scans) or InForm (for selected MSI fields) software.

Epinephrine dosing experiments and epinephrine ELISA

In indicated experiments, wild type mice were injected i.p. with 20 µg of Epinephrine dissolved in 200 µl of PBS and sacrificed 30 minutes after injection. 100 µl of whole blood was collected, processed, and assessed by flow cytometry. In separate experiments, mice were subjected to 30 minutes of exercise, then sacrificed 20 minutes after completion of exercise, and 200 µl of whole blood was collected. Sera was isolated from whole blood using a previously described centrifugation isolation[38], and subjected to Epinephrine ELISA detection kit (Novus Biologicals, CO).

Single Cell RNAseq Data Pre-Processing

Sequencing results were demultiplexed and converted to FASTQ format using Illumina bcl2fastq software. The Cell Ranger Single-Cell Software Suite (https://support.10xgenomics.com/single-cell-gene-expression/software/pipelines/latest/what-is-cell-ranger) was used to perform sample demultiplexing, barcode processing, and single-cell 3' gene counting. The cDNA insert was aligned to the mm10/GRCm38 reference genome. Only confidently mapped non-PCR duplicates with valid barcodes and UMIs were used to generate the gene-barcode matrix. Further analysis including the identification of highly variable genes, dimensionality reduction, standard unsupervised clustering algorithms, and the discovery of differentially expressed genes was performed using the *Seurat* R package[39,40]. To exclude low quality cells, cells that were extreme outliers in terms of library complexity, or cells that may possibly be multiple cells or doublets, we calculated the distribution of genes detected per cell and removed any cells in the top and bottom 2% quantiles. We additionally removed cells with more than 10% of the transcripts coming from mitochondrial genes.

Integrated Analysis of Single Cell Datasets

To account for technical batch differences between the three libraries, we utilized the Seurat alignment method for data integration, which specifically does not expect that confounding variables have uniform effects on all cells in a dataset and allows for global transcriptional shifts between datasets. Seurat uses a variant of canonical correlation analysis (CCA) to find linear combinations of features and identifies shared correlation structures across datasets. For each dataset, we identified variable genes, while controlling for the strong relationship between variability and average expression. We took the union of the top 2,000 genes with the highest

dispersion from both datasets and ran a CCA to determine the common sources of variation between datasets. We then aligned the subspaces based on the first 15 canonical correlation vectors, generating a new dimensionality reduction that was then used for further analysis. For single cell analysis of an unbiased pool of $CD45^+$ tumor-infiltrating leukocytes, we refined our analysis to include $CD45^+$ expressing cells that expressed >500 detected genes. We then normalized the data by the total expression, multiplied this by a scale factor of 10,000, and log-transformed the result. The final dataset included 4,216 cells with a median of 1,103 detected genes.

Visualization and Clustering of Single Cell RNAseq Data

To visualize the data, we further reduced the dimensionality of the dataset to project the cells in two-dimensional space using PCA followed by t-distributed Stochastic Neighbor Embedding (tSNE) based on the aligned CCA. Aligned CCA was also used as a basis for partitioning the dataset into clusters using a smart local moving (SLM) community detection algorithm (https://arxiv.org/ftp/arxiv/papers/1308/1308.6604.pdf). To find markers that define individual clusters, we performed differential expression analysis using Wilcoxon rank sum test for each cluster compared to all other cells for genes detected in at least 20% of the cluster cells. The initial analysis of PDA-infiltrating leukocytes yielded 16 clusters. We assigned cell type identities based on the expression of known population markers as follows: Cluster 1: CD8+ T cells – *CD8a* ^{hi} *CD3g* ^{hi} *Trbc2* ^{hi} *Gzmb* ^{hi} *Gzmk* ^{hi} *CD28* ^{hi} *CD74* ^{lo} ; Cluster 2: CD8+ T cells – *CD8a* ^{hi} *CD3g* ^{hi} *Trbc1* $^{h\,i}$ *Gzmb* ^{lo} *Gzmk* ^{lo} *Pdcd1* ^{hi} *Lag3*^{hi}; Cluster 3: Myeloid Suppressor Cells– *Hdc* ^{hi} *Mmp9* ^{hi} *Csf3r* ^{hi} *S100ap* ^{hi} *Fcgr3* ^{hi} *Ccrl2* ^{hi} *Cxcl2* ^{hi} *Itgam* ^{med} *Cd3g*^{neg}; Cluster 4: CD4+ T cells – *CD4* ^{hi} *Icos* ^{hi} *CD28* ^{hi} *CD3g* ^{hi} *Trbc2* ^{hi} *CD8a*^{lo} ; Cluster 5: NK Cells – *Klrb1c* ^{hi} *Klra8* ^{hi} *Klra9* ^{hi} *Gzma* ^{hi} *Klrc2* ^{hi} *Trbc2* ^{lo} *Eomes* ^{hi} *Ncr1* ^{hi} *Trbc2* ^{lo}; Cluster 6: B Cells – *CD79a* ^{hi} *Iglc2* ^{hi} *CD79b* ^{hi} *Ebf1* ^{hi} *CD19* ^{hi} *Igkc* ^{hi} *Trbc2* ^{lo} *Nkg7* ^{lo} *CD22* ^{hi} ; Cluster 7: CD4- CD8- T cells – *CD4* ^{neg} *CD8a* ^{lo} *Lef1* ^{hi} *Txk* ^{hi} *Trac* ^{med} *Trdc* ^{hi} *CD74* ^{lo}; Cluster 8: M2 Macrophages – *H2- Ab1*^{hi} *H2-Eb1* $^{\text{hi}}$ *C1qc* ^{hi} *C1qa/b* ^{hi} *Arg1* ^{hi} *Mmp12/13* ^{hi} *Apoe* ^{hi} *CD68* ^{hi} *CD74* ^{hi} *Nkg7* ^{lo} *CD8b1*^{lo}; Cluster 9: Dendritic Cells (P1) – *Clec9a* ^{hi} *Itgae* ^{hi} *Batf3* ^{hi} *PPt1* ^{hi} *Plet1* ^{hi} *Ifi205* ^{hi} *Flt3* ^{hi} *Tlr3*^{hi} ; Cluster 10: Monocyte/Macrophages – *Tgfbi* ^{hi} *Tlr2* ^{hi} *Ifitm6* ^{hi} *F13a1* ^{hi} *CCl9*^{hi} *CD14*^{hi} *Chil3*^{hi}; Cluster 11: Ductal/Tumor cells – *Cdk1*^{hi} *Mki67*^{hi} *Cdkn3*^{hi} *Cit*^{hi} *Cdca8*^{hi} *CCnb2* ^{hi} ; Cluster 12: Dendritic Cells (L) – *Ffar2*^{hi} *Epcam* ^{med} *Siglece* ^{med} *Batf3* ^{med} *Mgl2* ^{hi} *Kmo*^{hi}*;* Cluster 13: CD209 $^{\text{hi}}$ Myeloid Cells – *CD209a* ^{hi} *CD209d* ^{hi} *Ddr1* ^{hi}

Flt3 ^{hi} *Sgk3* ^{hi} *Clec10a* ^{hi}; Cluster 14: Myeloid Suppressor – *Mmp9* ^{hi} *CD33* ^{hi} *Il1rn* ^{hi} *Itgam* ^{med} *Cxcr2* ^{hi} *Trem1* ^{hi} *CD14* ^{hi} *Pilra* ^{hi} *Csf3r* ^{hi} *Cxcl2* ^{hi} *Hdc* ^{hi} ; Cluster 15: Dendritic Cells (L2) – *Cacnb3* ^{hi} *Fscn1* ^{hi} *Tmem123* ^{hi} *Ccl22* ^{hi} *Plek2* ^{hi} *Il12b* ^{hi} *CD3g* ^{lo} *CD3d* ^{lo}; Cluster 16: Dendritic Cells (P2) – *Siglech* ^{hi} *Lair1* ^{hi} *Upb1* ^{hi} *Klk1* ^{hi} *CD3d* ^{lo} *CD3g* ^{lo}. The raw gene counts data were used for further differential expression analysis. To identify the differentially expressed genes, *Seurat* R package was used. The resulting genes with adjusted $p<0.05$ were considered significant. To identify the signaling pathways in which genes are enriched, Ingenuity Pathway Analysis was carried out for genes that were considered significant. The canonical pathways analyzed in IPA software (Ingenuity Pathway Analysis, Qiagen) are represented as bar-plots.

Statistical Analysis

Data is presented as mean +/- standard error. Statistical significance was determined by the Student's *t* test using GraphPad Prism 7, where indicated (GraphPad Software, La Jolla, CA). p-values <0.05 were considered statistically significant.

Author Contributions:

(EK) – experimental design, manuscript preparation, project oversight, and experimental execution. (CAH) – experimental execution and design. (TD) experimental design and execution. (SAS) – experimental execution. (EV) – manuscript preparation and experimental design. (RW) – manuscript preparation and experimental design. (DBS) – experimental design, manuscript preparation, project oversight.

Acknowledgements:

The KPC cell line (line 4662) was a kind gift from Dr. R.H. Vonderheide. We would like to thank the New York University Langone Medical Center (NYULMC) Genome Technology Center (GTC) and Flow Cytometry Core each supported in part by the Laura and Isaac Perlmutter Cancer Center Support Grant P30CA016087 and by grant UL1 TR000038 from the National Center for the Advancement of Translational Science (NCATS). We specifically thank members of the Experimental Pathology Research Laboratory, which is partially supported by NIH/NCI 5 P30CA16087 (VM & CL) and S10 OD021747 (PerkinElmer/AkoyaBiosciences® Vectra® multispectral imaging system), for their technical support and expertise. E.K. was supported by

NIH/NCI grant F30 CA243205 and T32- GM136573. E.A. Vucic was supported by a Canadian Institutes of Health Research Fellowship (146792). This work was supported by NIH/NCI Grant CA210263 (D.B.-S).

Figure 1

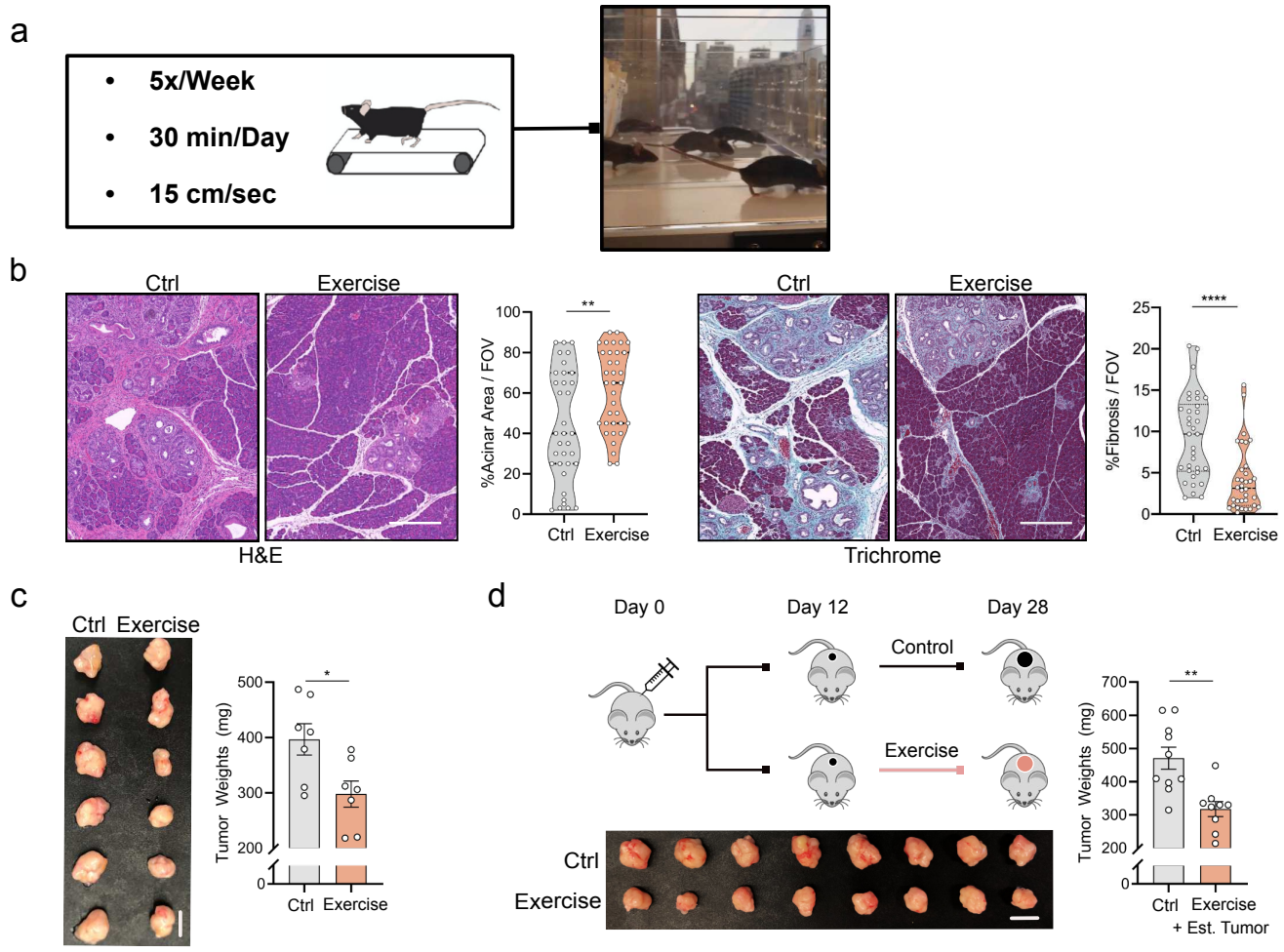

403

404 **Figure 1:** ***Aerobic exercise restricts pancreatic cancer growth and reduces tumor size***

405 **a**. The forced treadmill running model (aerobic exercise) is shown. The frequency, speed, and
406 duration of aerobic exercise are indicated (left). Representative photograph of mice running on the
407 treadmill is shown (right). **b**. 8-week old LSL-KRAS$^{G12D/WT}$; p48$^{Cre/WT}$ (KC) mice were exercised
408 (Exercise) for 6 weeks. Control mice remained sedentary. Mice were sacrificed at 14 weeks old.
409 Histologic staining of pancreata tissue sections with Hematoxylin and Eosin (H&E, left) and
410 Trichrome and Gomori (Trichrome, right) are shown. Representative images and quantification of
411 acinar (left) and fibrotic (right) areas are shown. Each dot represents quantification in one field of
412 view (FOV; 5-9 FOV analyzed from 3 tissue sections separated by at least 100 µm; n = 5 mice).
413 Scale bar represents 200 µm. **c.** 8-week old female C57BL/6J wild type mice (WT) were injected
414 orthotopically with 1x10^5 LSL-KRAS$^{G12D/WT}$; LSL-Trp53$^{R172H/WT}$; p48$^{Cre/WT}$ (KPC) 4662 cells
415 into the pancreas at Day 0 and exercise was started at Day 1. Control mice remained sedentary.
416 Mice were sacrificed at Day 21. Representative tumor images (left) and quantification of tumor

weights (right) are shown. Scale bar represents 1 cm. Each dot represents one tumor (n = 7). **d**. 8-week old female WT mice were injected orthotopically with $5x10^{\wedge 4}$ KPC 4662 cells into the pancreas at Day 0. At Day 12 following implantation, mice were randomized into control and exercise cohorts. Mice were sacrificed at Day 28. Schematic of experimental design (top), tumor images (bottom) and quantification of tumor weights (right) are shown. Scale bar represents 1 cm. Each dot represents one tumor (n = 9-10). ($p < 0.05$ = *, $p < 0.001$ = **, $p < 0.0001$ = ****).

Figure 2

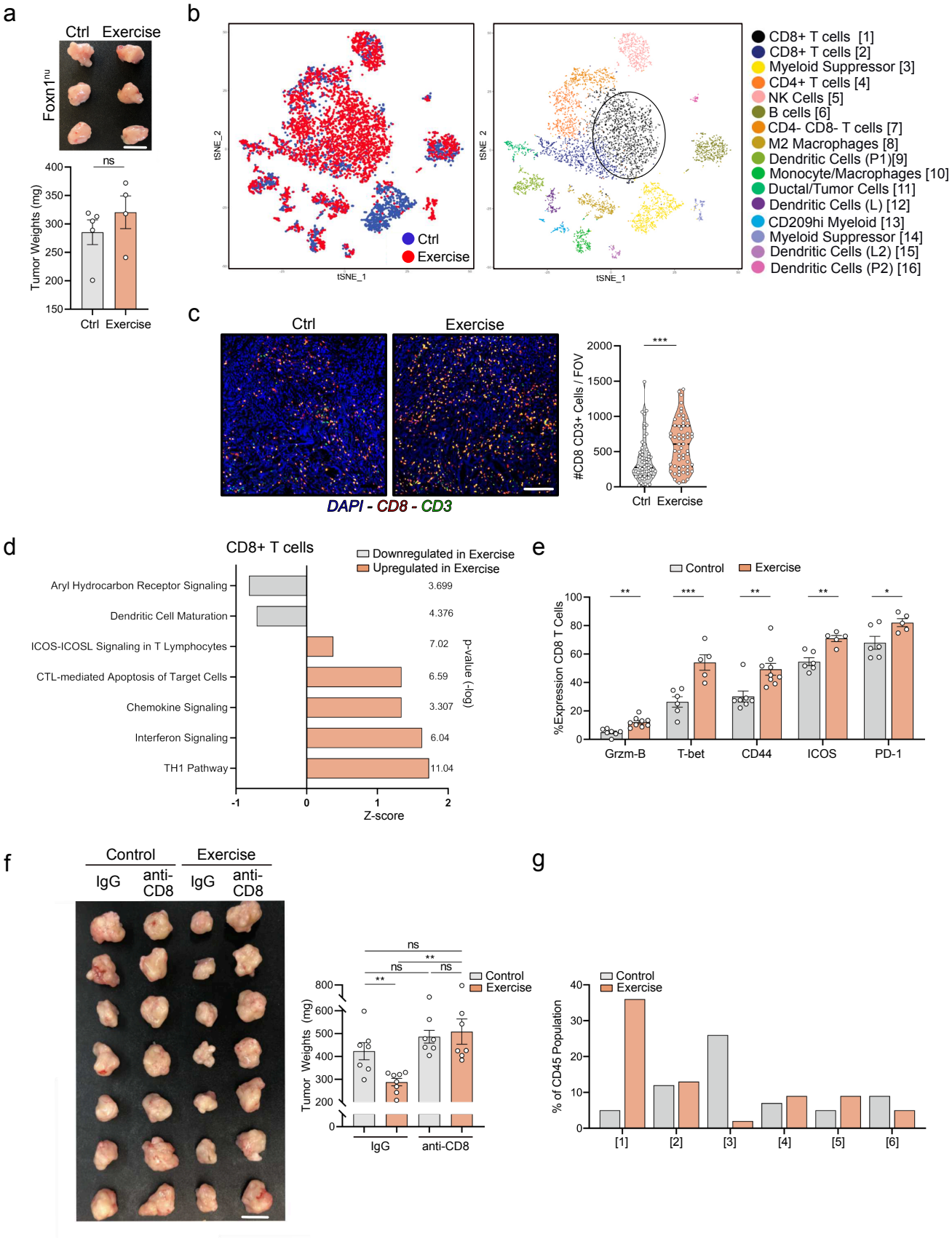
a
Ctrl
Exercise
Foxn1nu
ns
Tumor Weights (mg)
400
350
300
250
200
150
Ctrl
Exercise
b
tSNE_2
tSNE_1
Ctrl
Exercise
CD8+ T cells [1]
CD8+ T cells [2]
Myeloid Suppressor [3]
CD4+ T cells [4]
NK Cells [5]
B cells [6]
CD4- CD8- T cells [7]
M2 Macrophages [8]
Dendritic Cells (P1)[9]
Monocyte/Macrophages [10]
Ductal/Tumor Cells [11]
Dendritic Cells (L) [12]
CD209hi Myeloid [13]
Myeloid Suppressor [14]
Dendritic Cells (L2) [15]
Dendritic Cells (P2) [16]
c
Ctrl
Exercise
DAPI - CD8 - CD3
***
#CD8 CD3+ Cells / FOV
2000
1500
1000
500
0
Ctrl
Exercise
d
CD8+ T cells
Downregulated in Exercise
Upregulated in Exercise
Aryl Hydrocarbon Receptor Signaling
Dendritic Cell Maturation
ICOS-ICOSL Signaling in T Lymphocytes
CTL-mediated Apoptosis of Target Cells
Chemokine Signaling
Interferon Signaling
TH1 Pathway
3.699
4.376
7.02
6.59
3.307
6.04
11.04
p-value (-log)
-1
0
1
2
Z-score
e
Control
Exercise
%Expression CD8 T Cells
100
80
60
40
20
0
**
***
**
**
*
Grzm-B
T-bet
CD44
ICOS
PD-1
f
Control
Exercise
IgG
anti-CD8
IgG
anti-CD8
ns
**
ns
ns
**
Control
Exercise
Tumor Weights (mg)
800
600
500
400
300
200
0
IgG
anti-CD8
g
Control
Exercise
% of CD45 Population
40
30
20
10
0
[1]
[2]
[3]
[4]
[5]
[6]

Figure 2: ***The tumor protective effects of aerobic exercise are dependent on CD8 T cells***

a. 8 week old female athymic nude NU/J mice were injected orthotopically with $1x10^{\wedge 5}$ KPC 4662 cells at Day 0 and exercise was started at Day 1. Control mice remained sedentary. Mice were sacrificed at Day 21. Representative tumor images (top) and quantification of tumor weights (below) are shown. Scale bar represents 1 cm. Each dot represents one tumor (n =4-5). **b-g**. 8-week old female C57BL/6J wild type mice (WT) were injected orthotopically with $1x10^{\wedge 5}$ KPC 4662 cells into the pancreas at Day 0 and exercise was started at Day 1. Control mice remained sedentary. Mice were sacrificed at Day 21 and tumors analyzed as follows. **b**. Single cell RNASeq (scRNAseq) was performed on live leukocytes (PI-, CD45+) isolated by FACS. The distribution of cellular clusters was determined using the tSNE algorithm: control (blue) and exercise (red) leukocytes were identified (left), phenotypic clusters were identified by distinct colors (middle) and labeled (right) (n = 3 tumors pooled in each group). **c.** Tumor sections were stained by multiplex immunofluorescence for CD8 (red), CD3 (green), and DAPI (blue). The number of CD8+ CD3+ (yellow) cells were quantified in ImageJ. Each dot represents quantification in one field of view (13-16 FOV analyzed; n=4). Scale bar represents 75 μm. **d.** Upstream canonical pathway perturbations were derived using ingenuity pathway analysis. Pathways up-regulated (orange) or down-regulated (grey) in exercise were identified in the CD8+ T cell, Cluster 1. **e.** Single cell suspensions derived from tumors were stained with antibodies against CD45, CD3, CD4, CD8, Granzyme-B, T-bet, CD44, ICOS, and PD-1 and analyzed by flow cytometry. Each dot represents one tumor (n=6). **f.** Control and exercise mice were treated 3x/week with isotype or 200 μg of α-CD8 blocking antibody starting on Day 1. Tumor images (left) and quantification of tumor weights (right) are shown. Scale bar represents 1 cm. Each dot represents one tumor (n=7). **g.** Quantification of the relative proportion of the six most prominent immune populations in control and exercise tumors from scRNAseq. ($p > 0.05$ = ns, $p < 0.05$ = *, $p < 0.01$ = **, $p < 0.001$ = ***).

Figure 3

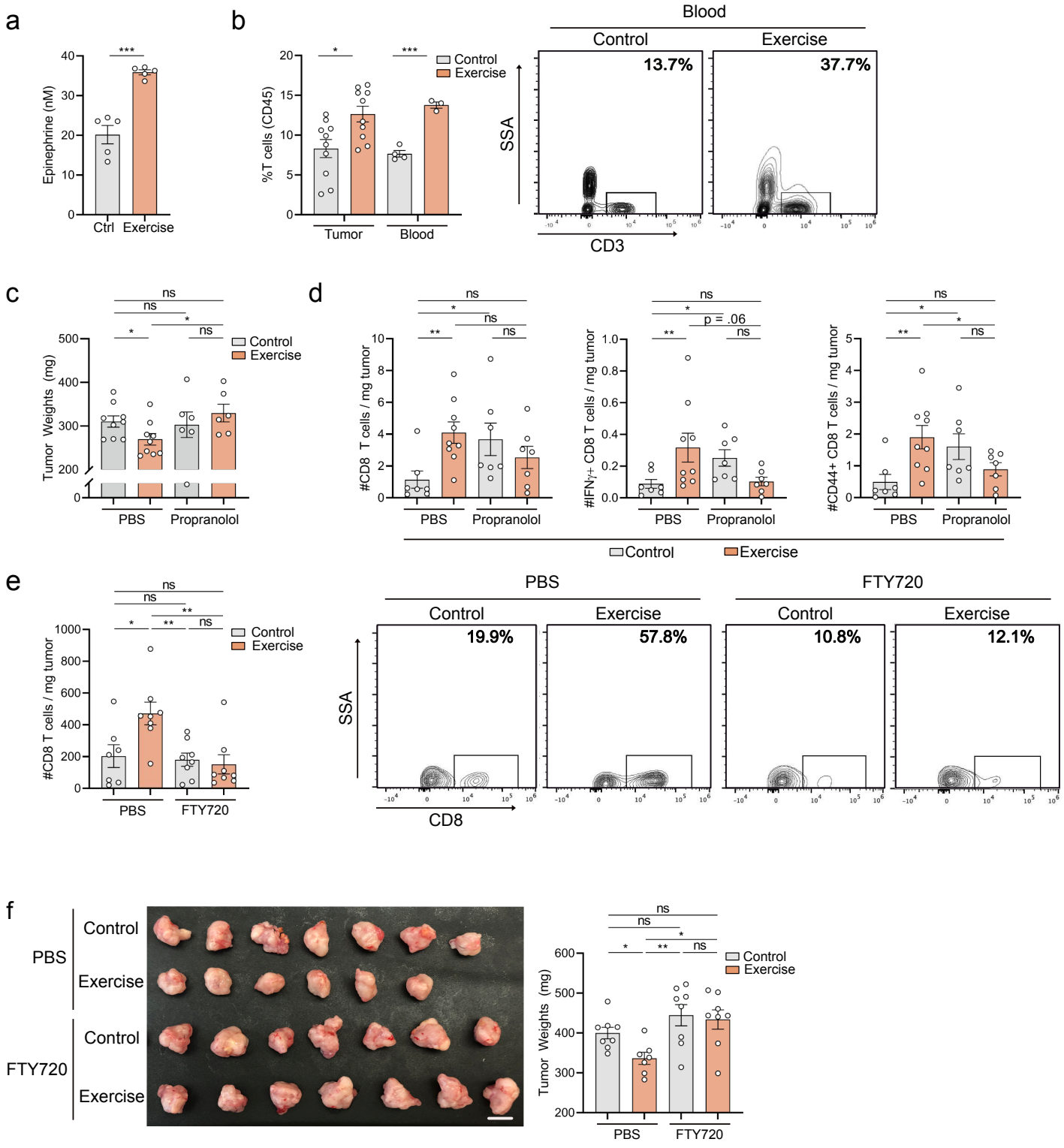
a
Epinephrine (nM)
Ctrl
Exercise
b
% T cells (CD45)
Control
Exercise
Tumor
Blood
Blood
Control
Exercise
13.7%
37.7%
SSA
CD3
c
Tumor Weights (mg)
PBS
Propranolol
d
#CD8 T cells / mg tumor
#IFNγ+ CD8 T cells / mg tumor
p = .06
#CD44+ CD8 T cells / mg tumor
e
#CD8 T cells / mg tumor
PBS
FTY720
PBS
FTY720
19.9%
57.8%
10.8%
12.1%
SSA
CD8
f
PBS
FTY720
Control
Exercise
Tumor Weights (mg)

Figure 3: ***Exercise-induced increase in intra-tumoral CD8 T cells is β-adrenergic and S1P-gradient dependent.***

a. 8 week-old female WT mice were exercised for 30 minutes at 15cm/sec and were sacrificed 20 minutes after completion of exercise. 200 µl of whole blood was collected, sera were isolated using centrifugation, and samples were subjected to ELISA for detection of Epinephrine levels. Each dot represents one mouse (n = 5). **b-f**. 8-week old female C57BL/6J wild type mice (WT) were injected orthotopically with 1x10^5 KPC 4662 cells into the pancreas at Day 0 and exercise was started at Day 1. Control mice remained sedentary. **b.** Mice were sacrificed at Day 21, thirty minutes after completion of exercise, and tumors and whole blood were harvested, digested, and assessed for relative numbers of CD3+ T cells. Each dot represents one mouse (n =3-4 each for blood, n= 10 for tumors). Representative contour plots are shown for CD3+ cells as a percentage of CD45+ cells in whole blood. **c-d.** Mice were provided with either normal drinking water or .5g/L propranolol drinking water ad libitum starting on Day 1. Mice were sacrificed on Day 21 and tumor weights were quantified (c), and single cell suspensions derived from tumors were stained with antibodies against CD45, CD3, CD8, IFNγ, and CD44 and analyzed by flow cytometry (d). Each dot represents one tumor (n= 6-9). **e-f.** Mice were treated daily either with PBS or 200 µl of fingolimod (FTY720) starting on Day 1. Mice were sacrificed at Day 21. Single cell suspensions derived from tumors were stained with antibodies against CD45, TCRB, CD4, and CD8, and analyzed by flow cytometry. Each dot represents one tumor. Representative flow cytometry plots are shown for CD8+ cells as fraction of CD4– CD3+ cells (e). Tumor images (left) and quantification of tumor weights (right) are shown (f). Scale bar represents 1 cm. Each dot represents one tumor (n =7). ($p > 0.05$ = ns, $p < 0.05$ = *, $p < 0.01$ = **, $p < 0.001$ = ***).

Figure 4

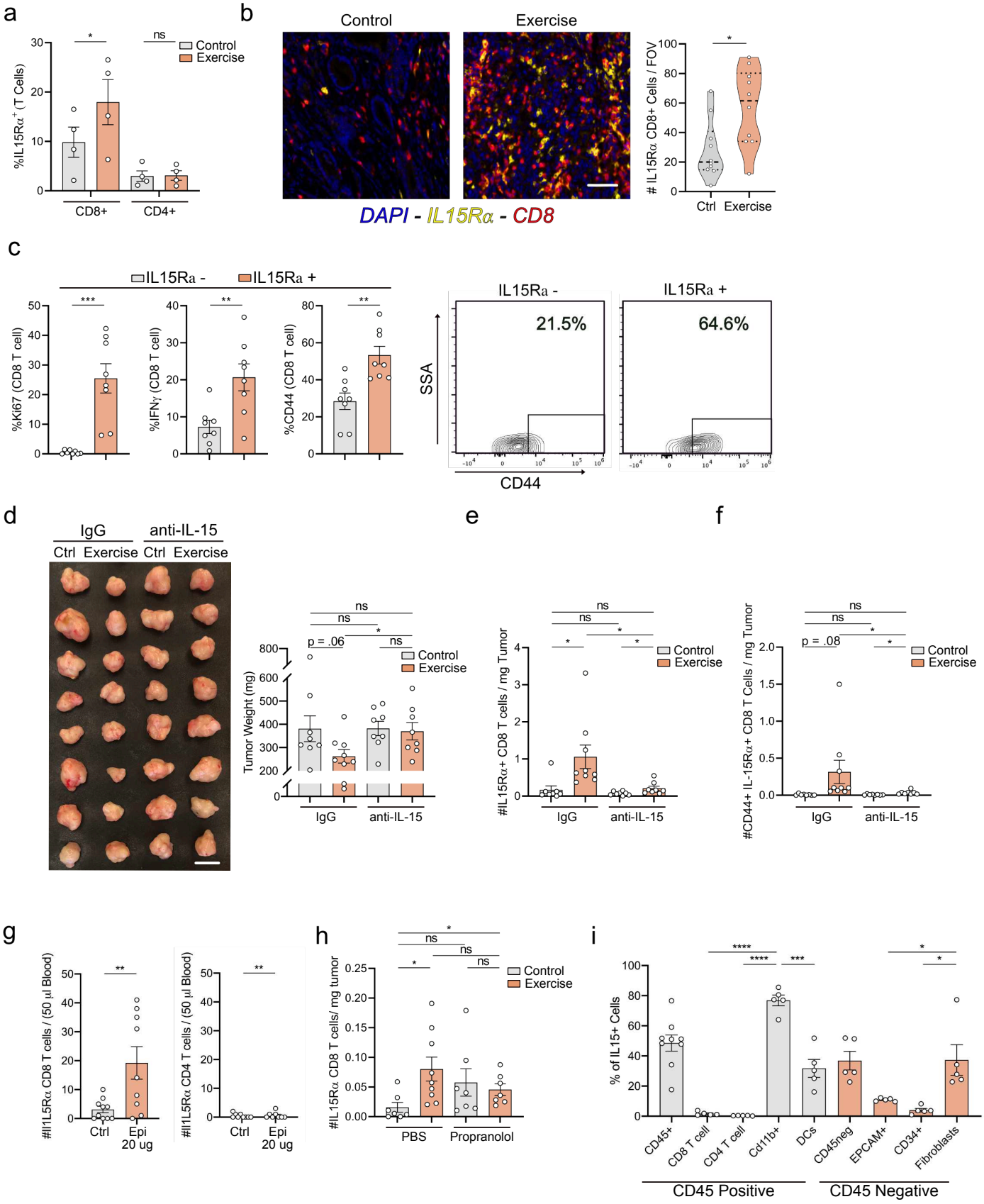
a
b
c
d
e
f
g
h
i
Control
Exercise
ns
%IL15Rα+ (T Cells)
CD8+
CD4+
DAPI - IL15Rα - CD8
IL15Rα CD8+ Cells / FOV
Ctrl
IL15Ra -
IL15Ra +
%Ki67 (CD8 T cell)
%IFNγ (CD8 T cell)
%CD44 (CD8 T cell)
21.5%
64.6%
SSA
CD44
IgG
anti-IL-15
Tumor Weight (mg)
p = .06
#IL15Rα+ CD8 T cells / mg Tumor
#CD44+ IL-15Rα+ CD8 T Cells / mg Tumor
p = .08
#Il1L5Rα CD8 T cells / (50 µl Blood)
#Il1L5Rα CD4 T cells / (50 µl Blood)
Epi 20 ug
#IL15Rα CD8 T cells/ mg tumor
PBS
Propranolol
% of IL15+ Cells
CD45+
CD8 T cell
CD4 T cell
Cd11b+
DCs
CD45neg
EPCAM+
CD34+
Fibroblasts
CD45 Positive
CD45 Negative

Figure 4: IL-15/IL15Rα axis is required for exercise-mediated tumor protection

a-f. 8-week old female C57BL/6J wild type mice (WT) were injected orthotopically with 1x10^5 KPC 4662 cells into the pancreas at Day 0 and exercise was started at Day 1. Control mice remained sedentary. Mice were sacrificed at Day 21 and tumors analyzed as follows. **a.** Single cell suspensions derived from tumors were stained with antibodies against CD45, CD3, CD4, CD8, and IL-15Rα and analyzed by flow cytometry. Each dot represents one tumor (n=4). **b.** Tumor sections were stained by multiplex immunofluorescence for CD8 (red), IL-15Rα (yellow), and DAPI (blue). The number of CD8+ IL-15Rα+ (orange) cells were quantified in ImageJ. Each dot represents quantification per field of view (3-4 FOV analyzed; n=3). Scale bar represents 40 μm. **c.** Single cell suspensions derived from tumors were stained with antibodies against CD8, Ki67, IFNγ, CD44 and IL-15Rα and analyzed by flow cytometry. Each dot represents one tumor (n=8). Representative flow cytometry plots are shown for CD44. **d-f.** Mice were treated 3x/week with isotype or 200 μg of α-IL15 neutralizing antibody starting on Day 1 post-op. Tumor images (left) and quantification of tumor weights (right) are shown. Scale bar represents 1 cm (d). Single cell suspensions derived from tumors were stained and analyzed by flow cytometry for number of IL-15Rα+ CD8+ T cells (e) and CD44+ IL-15Rα+ CD8+ T cells (f). Each dot represents one tumor (n=8-9). **g.** 9-week-old female WT mice were injected i.p. with PBS or 20 μg of Epinephrine. Thirty minutes post-treatment 100 μl of whole blood was isolated and assessed by flow cytometry for number of IL-15Rα+ CD8+ T cells (left) or IL-15Rα+ CD4+ T cells (right). Each dot represents one mouse (n =9-10). **h.** 8-week old female C57BL/6J wild type mice (WT) were injected orthotopically with 1x10^5 KPC 4662 cells into the pancreas at Day 0 and exercise was started at Day 1. Control mice remained sedentary. Mice were provided either normal drinking water or .5g/L propranolol drinking water ad libitum starting on Day 1. Mice were sacrificed at Day 21. Single cell suspensions derived from tumors were assessed by flow cytometry for number of IL-15Rα+ CD8+ T cells. Each dot represents one tumor (n= 6-9). **i.** 8-week old female C57BL/6J wild type mice (WT) were injected orthotopically with 1x10^5 KPC 4662 cells into the pancreas at Day 0. All mice remained sedentary. Single cell suspensions derived from tumors were stained with antibodies against CD45, CD3, CD8 T cells (CD8+ CD3+), CD4 T cells (CD4+ CD3+), CD11b, DCs (CD11c+ MHCII hi), EPCAM, CD34, Fibroblasts (CD140a+ CD34- EPCAM-CD45-) and analyzed by flow cytometry for the expression of IL-15. Each dot represents one tumor (n=5-9). ($p > 0.05$ = ns, $p < 0.05$ = *, $p < 0.01$ = **, $p < 0.001$ = ***, $p < 0.0001$ = ****).

Figure 5

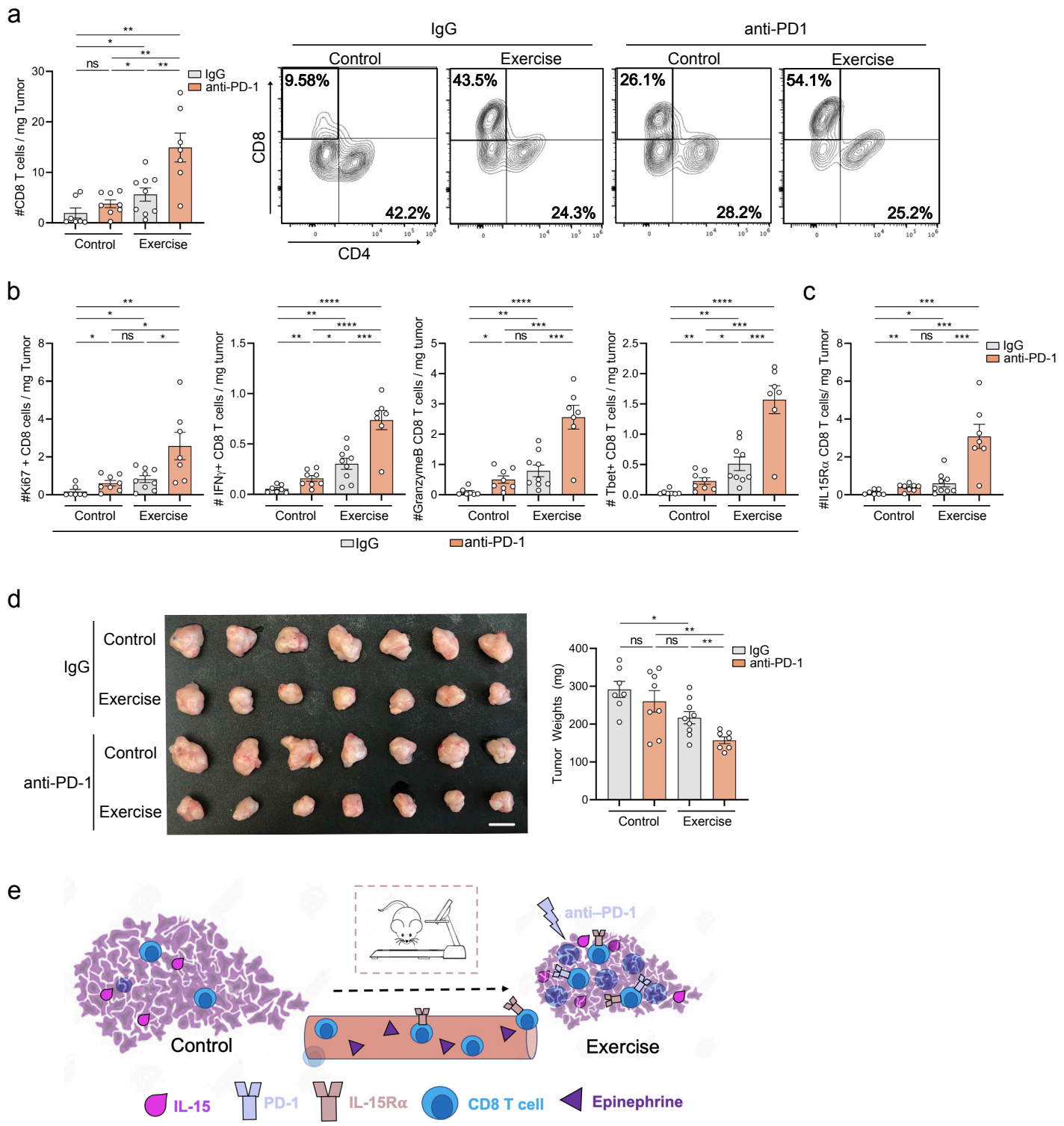

Figure 5: Aerobic Exercises Sensitizes Pancreatic Cancer to anti-PD1 Immunotherapy

a-d. 8-week old female C57BL/6J wild type mice (WT) were injected orthotopically with 1x10^5 KPC 4662 cells into the pancreas at Day 0 and exercise was started at Day 1. Control mice

remained sedentary. Mice were treated 3x/week with isotype or 200 μg of α-PD-1 blocking antibody starting on Day 3. Mice were sacrificed at Day 21. Single cell suspensions derived from tumors were assessed by flow cytometry for CD3, CD4, and CD8 (a), for Ki67, Granzyme-B, T-bet, and IFNγ expression on CD8 T cells (b) and number of IL-15Rα+ CD8+ T cells (c). Tumor images (left) and quantification of tumor weights (right) are shown (d). Scale bar represents 1 cm. Each dot represents one tumor (n=7-8). **e.** Schematic depicting proposed mechanism for the impact of aerobic exercise on CD8 T cell mobilization, pancreatic tumor growth and anti-tumor immunity. ($p > 0.05$ = ns, $p < 0.05$ = *, $p < 0.01$ = **, $p < 0.001$ = ***, $p < 0.0001$ = ****).

Extended Data Figure 1

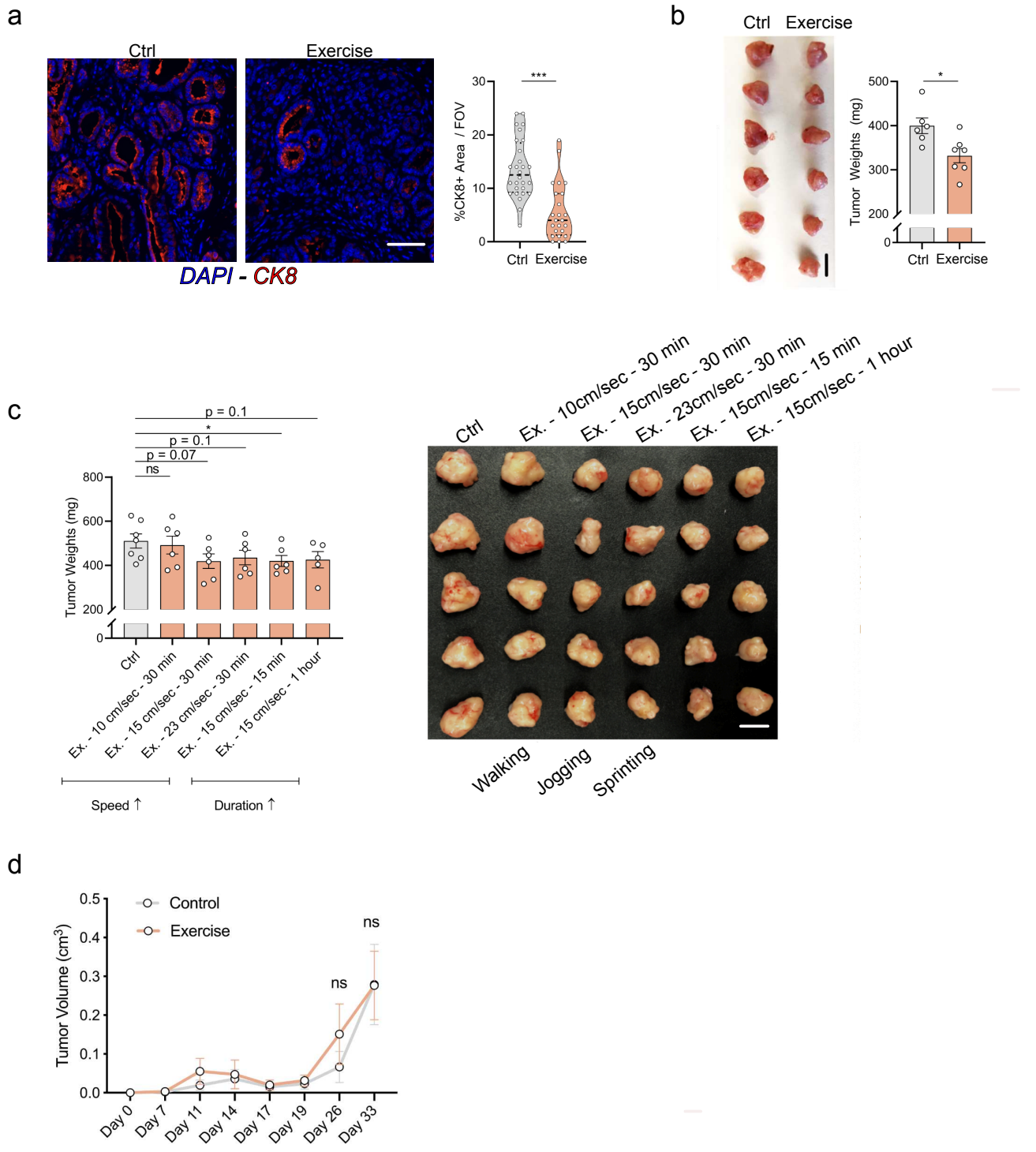

582 ***Extended Data Figure 1: Aerobic exercise restricts pancreatic cancer growth in a non-dose***
583 ***dependent manner***

584 **a.** 8-week old LSL-KRAS$^{G12D/WT}$; p48$^{Cre/WT}$ (KC) mice were exercised (Exercise) for 6 weeks.
585 Control mice remained sedentary. Mice were sacrificed at 14 weeks old. Histologic staining of
586 pancreata tissue sections with CK8 (red) and DAPI (blue) are shown. Quantification of the %

CK8+ of total DAPI positive cells per FOV was performed in ImageJ. Each dot represents quantification in one field of view (8 FOV, n = 3 mice). Scale bar represents 200 μm. **b.** 8-week old female C57BL/6J wild type mice (WT) were injected orthotopically with $1x10^{\wedge 5}$ cells of a second independent KPC cell line, KPC 1203, into the pancreas at Day 0 and exercise was started at Day 1. Control mice remained sedentary. Mice were sacrificed at Day 21 and tumors were harvested. Representative tumor images (left) and quantification of tumor weights (right) are shown. Scale bar represents 1 cm. Each dot represents one tumor (n =6-7). **c.** 8-week old female C57BL/6J wild type mice (WT) were injected orthotopically with $1x10^{\wedge 5}$ KPC 4662 cells into the pancreas at Day 0 and specified exercise regimen was started at Day 1. Control mice remained sedentary. Mice were sacrificed at Day 21 and tumors were harvested. Representative tumor images (right) and quantification of tumor weights (left) are shown. Scale bar represents 1 cm. Each dot represents one tumor (n=5). **d.** 8 week old WT mice were injected subcutaneously with $1x10^{\wedge 6}$ KPC FC1242 cells at Day 0 and exercise was started at Day 1. Control mice remained sedentary. Tumor volumes were measured using calipers at 3-7 day intervals. Each dot represents an average of five mice in each arm. ($p > 0.05$ = ns, $p < 0.05$ = *, $p < 0.001$ = ***).

Extended Data Figure 2

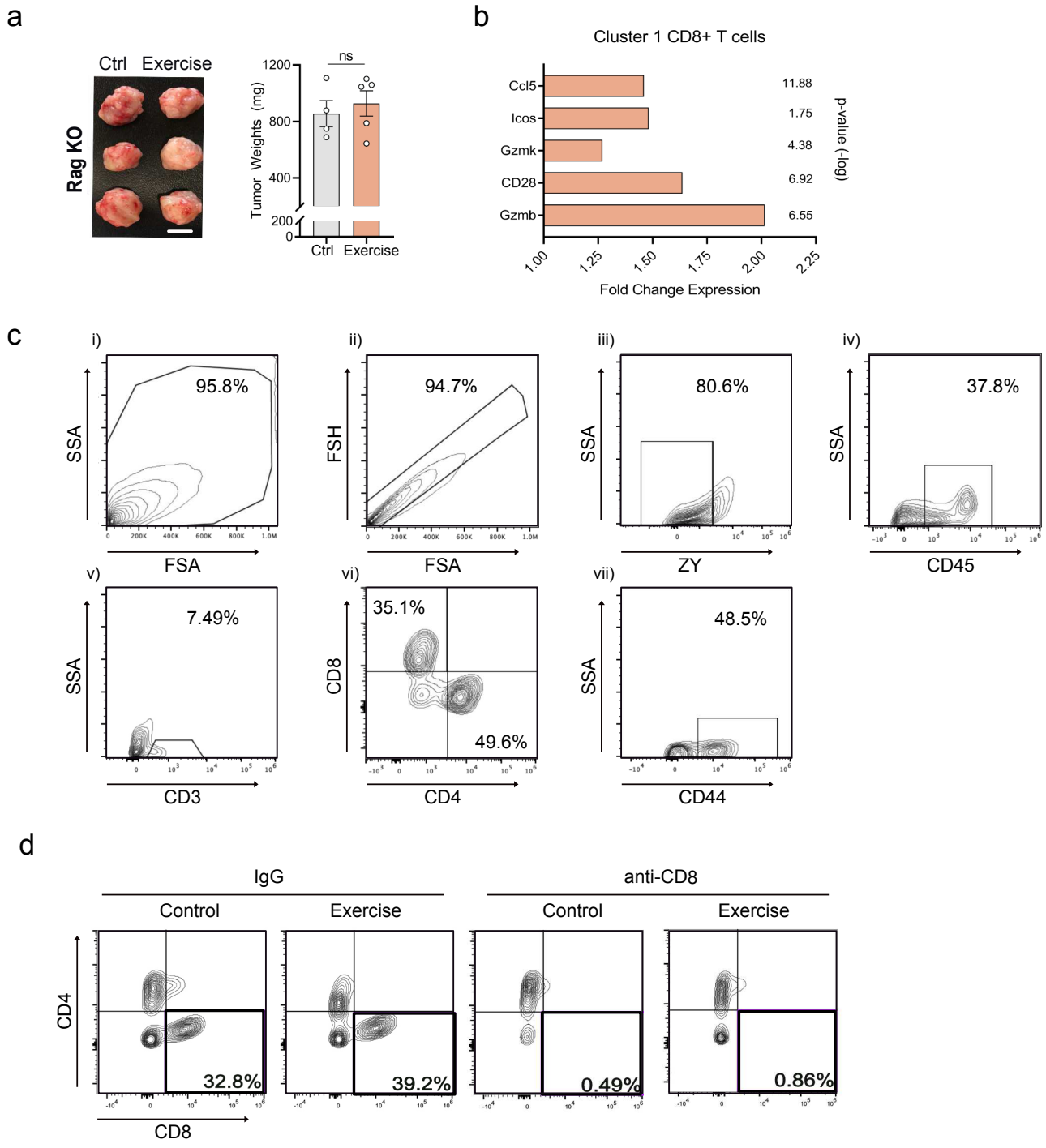

617

618 ***Extended Data Figure 2: Exercise-mediated tumor protection is CD8 T cell dependent***

619 **a.** 8 week old male RAG1KO mice were injected orthotopically with 1x10^5 KPC 4662 cells at
620 Day 0 and exercise was started at Day 1. Control mice remained sedentary. Mice were sacrificed
621 at Day 21. Representative tumor images (left) and quantification of tumor weights (right) are
622 shown. Scale bar represents 1 cm. Each dot represents one tumor (n =4-5). **b.** Gene expression

analysis of CD8+ T cells, Cluster 1 from scRNAseq of exercised tumors showing fold change of expression levels of Ccl5, Icos, Gzmk, Cd28, and Gzmb, relative to cells in other clusters. **c.** Representative contour plots indicating example gating strategy used for flow cytometry analysis, from top left: i) all cells in frame, ii) double-singlet discrimination, iii) live cells by zombie yellow (ZY) negative, iv) all immune cells (CD45+), v) T cells (CD3+), vi) CD8+ T cells (CD4 negative, CD8 positive, upper left quadrant), vii) expression level of CD44. **d.** Control and exercise mice were treated 3x/week with isotype or 200 μg of α-CD8 blocking antibody starting on Day 1. Mice were sacrificed at Day 21. Single cell suspension derived from tumors were assessed by flow cytometry for CD3, CD4, and CD8. Representative contour plots are shown for CD8+ CD4- cells as a fraction of total CD3 positive cells. ($p > 0.05$ = ns).

Extended Data Figure 3

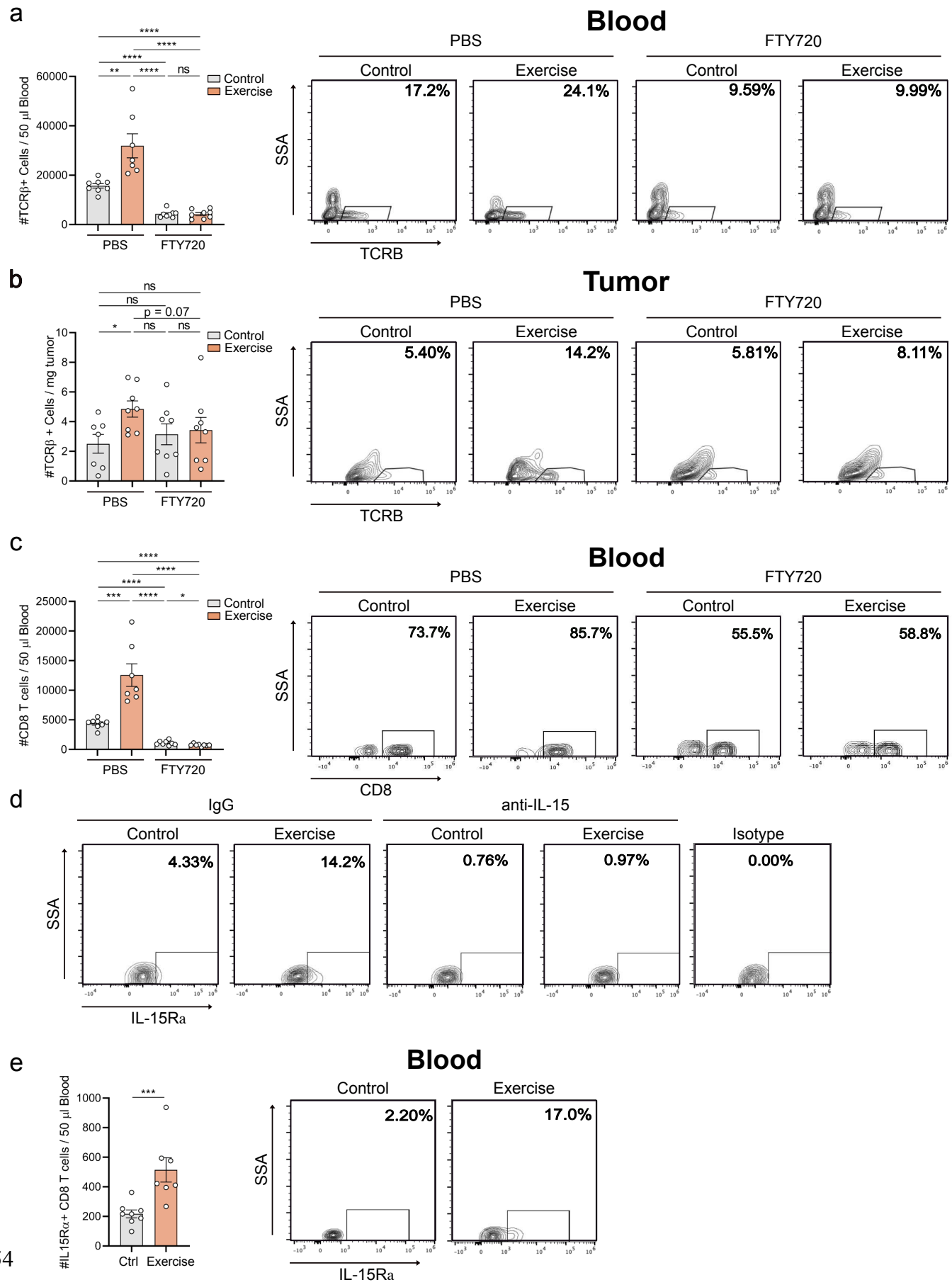

Extended Data Figure 3: Exercise-mediated increase in CD8 T cells is reversed with FTY720 / IL15Rα+ CD8 T cells are required for exercise-induced tumor protection

a-c. 8-week old female C57BL/6J wild type mice (WT) were injected orthotopically with 1x10^5 KPC 4662 cells into the pancreas at Day 0 and exercise was started at Day 1. Control mice remained sedentary. Mice were treated daily either with PBS or 200 µl of fingolimod (FTY720) starting on Day 1. Mice were sacrificed at Day 21. Single cell suspensions derived from whole blood or tumors were stained with antibodies against CD45, TCRB, CD4, and CD8, and analyzed by flow cytometry. Representative contour plots are shown for TCRB in blood (a), TCRB in tumor (b), and CD8 T cells in blood (c). Each dot represents one mouse (n=7) **d.** 8-week old female WT mice were injected orthotopically with 1x10^5 KPC 4662 cells into the pancreas at Day 0 and exercise was started at Day 1. Control mice remained sedentary. Mice were treated 3x/week with isotype or 200 µg of α-IL15 neutralizing antibody starting on Day 1 post-op. Single cell suspensions derived from tumors were stained with antibodies against CD8 and IL-15Rα and analyzed by flow cytometry. Representative contour plots for IL15Rα+ of total CD8+ cells, with staining isotype, are shown. **e.** 8-week old female WT mice were injected orthotopically with 1x10^5 KPC 4662 cells into the pancreas at Day 0 and exercise was started at Day 1. Control mice remained sedentary. Mice were sacrificed at Day 21, thirty minutes after completion of exercise and whole blood was harvested, digested, and assessed for relative numbers of IL15Rα+ CD8+ cells. Each dot represents one mouse (n=7). Representative contour plots are shown. ($p > 0.05$ = ns, $p < 0.05$ = *, $p < 0.01$ = **, $p < 0.001$ = ***, $p < 0.0001$ = ****).

Extended Data Figure 4

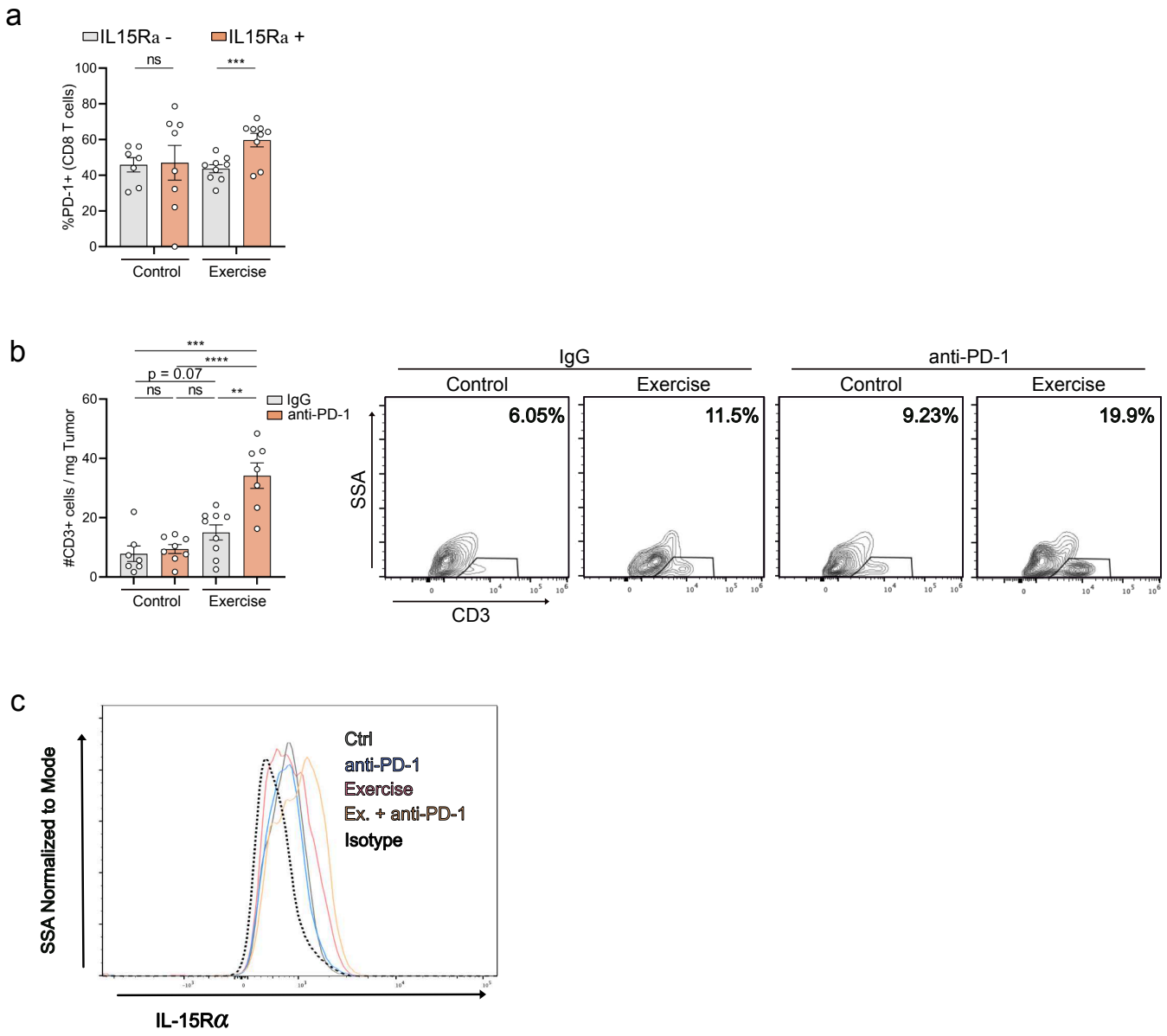

685

686 ***Extended Data Figure 4: Aerobic exercise and anti-PD-1 blockade exhibit intra-tumoral***
687 ***immunological synergy***

688 **a.** 8-week old female C57BL/6J wild type mice (WT) were injected orthotopically with 1x10^5
689 KPC 4662 cells into the pancreas at Day 0 and exercise was started at Day 1. Control mice
690 remained sedentary. Mice were sacrificed at Day 21 and tumors were harvested**.** Single cell
691 suspensions derived from tumors were stained with antibodies against CD3, CD8, PD-1 and IL-
692 15Rα and analyzed by flow cytometry. Each dot represents one tumor (n=7). **b-c.** 8-week old
693 female C57BL/6J wild type mice (WT) were injected orthotopically with 1x10^5 KPC 4662 cells
694 into the pancreas at Day 0 and exercise was started at Day 1. Control mice remained sedentary.

Mice were treated 3x/week with isotype or 200 μg of α-PD-1 blocking antibody starting on Day 3. Mice were sacrificed at Day 21. Single cell suspension derived from tumors were assessed by flow cytometry for CD3 (b), CD8, and IL15Rα+ (c). Each dot represents one tumor (n=7-8) Representative histogram plot is shown for IL15Rα+ in CD8 T cells. ($p > 0.05$ = ns, $p < 0.01$ = **, $p < 0.001$ = ***, $p < 0.0001$ = ****).

References:

1. Brown JC, Winters-Stone K, Lee A, Schmitz KH. Cancer, physical activity, and exercise. *Compr Physiol*. 2012;2(4):2775-2809. doi:10.1002/cphy.c120005.

2. Kenfield, S. A., Stampfer, M. J., Giovannucci, E. & Chan, J. M. Physical Activity and Survival After Prostate Cancer Diagnosis in the Health Professionals Follow-Up Study. *J Clin Oncol* **29**, 726–732 (2011).

3. Schmid, D. & Leitzmann, M. F. Association between physical activity and mortality among breast cancer and colorectal cancer survivors: a systematic review and meta-analysis. *Ann Oncol* **25**, 1293–1311 (2014).

4. Liu, L. *et al.* Leisure time physical activity and cancer risk: evaluation of the WHO's recommendation based on 126 high-quality epidemiological studies. *Brit J Sport Med* **50**, 372 (2016).

5. Jones, L. W. *et al.* Exercise and Prognosis on the Basis of Clinicopathologic and Molecular Features in Early-Stage Breast Cancer: The LACE and Pathways Studies. *Cancer Res***76**, 5415–5422 (2016).

6. Rundqvist, H. *et al.* Cytotoxic T-cells mediate exercise-induced reductions in tumor growth. *Elife* **9**, e59996 (2020).

7. Schadler, K. L. *et al.* Tumor vessel normalization after aerobic exercise enhances chemotherapeutic efficacy. *Oncotarget* **7**, 65429–65440 (2016).

8. Bedoya, C. A. F. *et al.* Exercise during preoperative therapy increases tumor vascularity in pancreatic tumor patients. *Sci Rep-uk* **9**, 13966 (2019).

9. Pedersen, L. *et al.* Voluntary Running Suppresses Tumor Growth through Epinephrine- and IL-6-Dependent NK Cell Mobilization and Redistribution. *Cell Metab* **23**, 554–562 (2016).

10. Ashcraft, K. A., Peace, R. M., Betof, A. S., Dewhirst, M. W. & Jones, L. W. Efficacy and Mechanisms of Aerobic Exercise on Cancer Initiation, Progression, and Metastasis: A Critical Systematic Review of In Vivo Preclinical Data. *Cancer Res***76**, 4032–4050 (2016).

11. Estruel-Amades, S., Camps-Bossacoma, M., Massot-Cladera, M., Pérez-Cano, F. J. & Castell, M. Alterations in the innate immune system due to exhausting exercise in intensively trained rats. *Sci Rep-uk* **10**, 967 (2020).

12. Tseng, W. W. *et al.* Development of an Orthotopic Model of Invasive Pancreatic Cancer in an Immunocompetent Murine Host. *Clin Cancer Res* **16**, 3684–3695 (2010).

13. Campbell, J. P. & Turner, J. E. Debunking the Myth of Exercise-Induced Immune Suppression: Redefining the Impact of Exercise on Immunological Health Across the Lifespan. *Front Immunol* **9**, 648 (2018).

14. Shek, P., Sabiston, B., Buguet, A. & Radomski, M. Strenuous Exercise and Immunological Changes. *Int J Sports Med* **16**, 466–474 (1995).

15. Bayne, L. J. *et al.* Tumor-Derived Granulocyte-Macrophage Colony-Stimulating Factor Regulates Myeloid Inflammation and T Cell Immunity in Pancreatic Cancer. *Cancer Cell* **21**, 822–835 (2012).

16. Siret, C. *et al.* Deciphering the Crosstalk Between Myeloid-Derived Suppressor Cells and Regulatory T Cells in Pancreatic Ductal Adenocarcinoma. *Front Immunol* **10**, 3070 (2020).

17. Pylayeva-Gupta, Y., Lee, K. E., Hajdu, C. H., Miller, G. & Bar-Sagi, D. Oncogenic Kras-Induced GM-CSF Production Promotes the Development of Pancreatic Neoplasia. *Cancer Cell* **21**, 836–847 (2012).

18. Krüger, K., Lechtermann, A., Fobker, M., Völker, K. & Mooren, F. C. Exercise-induced redistribution of T lymphocytes is regulated by adrenergic mechanisms. *Brain Behav Immun* **22**, 324–338 (2008).

19. Foster, N. K. *et al.* Leukocytosis of exercise: role of cardiac output and catecholamines. *Journal of Applied Physiology,* **18AD**, (1986).

20. Dimitrov, S., Lange, T. & Born, J. Selective Mobilization of Cytotoxic Leukocytes by Epinephrine. *J Immunol* **184**, 503–511 (2010).

21. Chiba, K. FTY720, a new class of immunomodulator, inhibits lymphocyte egress from secondary lymphoid tissues and thymus by agonistic activity at sphingosine 1-phosphate receptors. *Pharmacol Therapeut* **108**, 308–319 (2005).

22. Ruane, D. *et al.* Lung dendritic cells induce migration of protective T cells to the gastrointestinal tractLung dendritic cells' intestinal homing. *J Exp Medicine* **210**, 1871–1888 (2013).

23. Chiba, K. FTY720, a Novel Immunosuppressant, Induces Sequestration of Circulating Mature Lymphocytes by Acceleration of Lymphocyte Homing in Rats. *Journal of Immunology* (1998).

24. Pedersen, B. K., Åkerström, T. C. A., Nielsen, A. R. & Fischer, C. P. Role of myokines in exercise and metabolism. *J Appl Physiol* **103**, 1093–1098 (2007).

25. Idorn, M. & Hojman, P. Exercise-Dependent Regulation of NK Cells in Cancer Protection. *Trends Mol Med* **22**, 565–577 (2016).

26. Berard, M., Brandt, K., Paus, S. B. & Tough, D. F. IL-15 Promotes the Survival of Naive and Memory Phenotype CD8+ T Cells. *J Immunol* **170**, 5018–5026 (2003).

27. Lu, J. Interleukin 15 Promotes Antigen-independent in Vitro Expansion and Long-Term Survival of Antitumor Cytotoxic T Lymphocytes1. *Clinical Cancer Research* **8**, 3877–3884 (2002).

28. Wu, J. *et al.* Skeletal muscle antagonizes antiviral CD8+ T cell exhaustion. *Sci Adv* **6**, eaba3458 (2020).

29. Carrero, R. M. S. *et al.* IL-15 is a component of the inflammatory milieu in the tumor microenvironment promoting antitumor responses. *Proc National Acad Sci***116**, 201814642 (2018).

30. Marschner, N. *et al.* Association of Disease Progression with Health-Related Quality of Life Among Adults with Breast, Lung, Pancreatic, and Colorectal Cancer. *Jama Netw Open* **3**, e200643 (2020).

31. Yang, A. *et al.* Autophagy sustains pancreatic cancer growth through both cell autonomous and non-autonomous mechanisms. *Cancer Discov* **8**, CD-17-0952 (2018).

32. Grasselly, C. *et al.* The Antitumor Activity of Combinations of Cytotoxic Chemotherapy and Immune Checkpoint Inhibitors Is Model-Dependent. *Front Immunol***9**, 2100 (2018).

33. Meyer, M. A. & DeNardo, D. G. Better Together: B7S1 Checkpoint Blockade Synergizes with anti-PD1. *Immunity***48**, 621–623 (2018).

34. IL Li, H. Y. *et al.* The Tumor Microenvironment Regulates Sensitivity of Murine Lung Tumors to PD-1/PD-L1 Antibody Blockade. *Cancer Immunol Res* **5**, 767–777 (2017).

35. Ramos-Perez, W. D., Fang, V., Escalante-Alcalde, D., Cammer, M. & Schwab, S. R. A map of the distribution of sphingosine 1-phosphate in the spleen. *Nat Immunol* **16**, 1245–1252 (2015).

36. Pedersen, L. *et al.* Voluntary Running Suppresses Tumor Growth through Epinephrine- and IL-6-Dependent NK Cell Mobilization and Redistribution. *Cell Metab* **23**, 554–562 (2016).

37. Jaatinen, T. & Laine, J. Isolation of Mononuclear Cells from Human Cord Blood by Ficoll-Paque Density Gradient. *Curr Protoc Stem Cell Biology* **1**, 2A.1.1-2A.1.4 (2007).

38. Tuck, M. K. *et al.* Standard Operating Procedures for Serum and Plasma Collection: Early Detection Research Network Consensus Statement Standard Operating Procedure Integration Working Group. *J Proteome Res* **8**, 113–117 (2009).

39. Butler, A., Hoffman, P., Smibert, P., Papalexi, E. & Satija, R. Integrating single-cell transcriptomic data across different conditions, technologies, and species. *Nat Biotechnol* **36**, 411–420 (2018).

40. Stuart, T. *et al.* Comprehensive Integration of Single-Cell Data. *Cell* **177**, 1888-1902.e21 (2019).

Figures

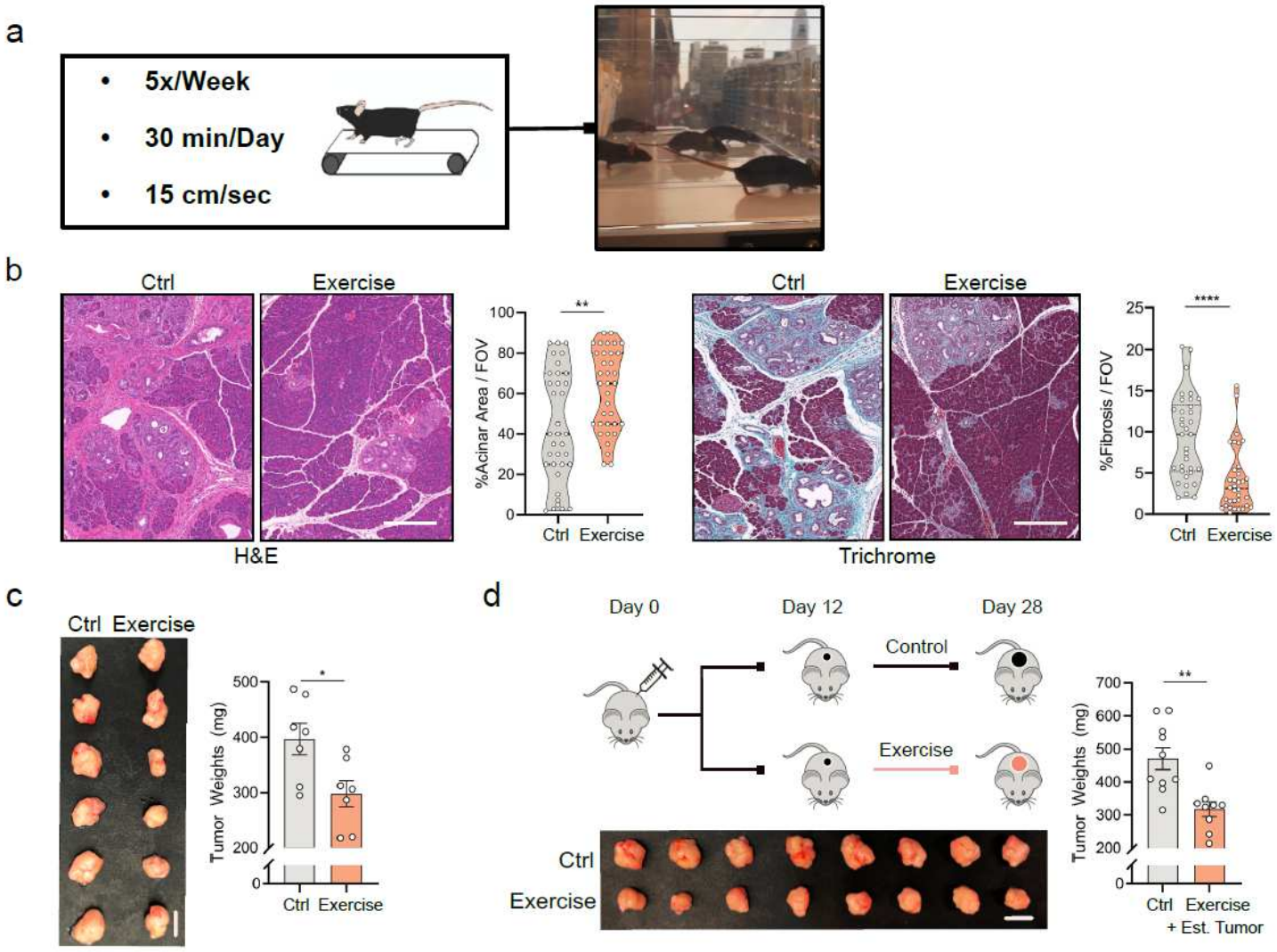

Figure 1

Aerobic exercise restricts pancreatic cancer growth and reduces tumor size a. The forced treadmill running model (aerobic exercise) is shown. The frequency, speed, and duration of aerobic exercise are indicated (left). Representative photograph of mice running on the treadmill is shown (right). b. 8-week old LSL-KRASG12D/WT; p48Cre/WT (KC) mice were exercised (Exercise) for 6 weeks. Control mice remained sedentary. Mice were sacrificed at 14 weeks old. Histologic staining of pancreata tissue sections with Hematoxylin and Eosin (H&E, left) and Trichrome and Gomori (Trichrome, right) are shown. Representative images and quantification of acinar (left) and fibrotic (right) areas are shown. Each dot represents quantification in one field of view (FOV; 5-9 FOV analyzed from 3 tissue sections separated by at least 100 μm; n = 5 mice). Scale bar represents 200 μm. c. 8-week old female C57BL/6J wild type mice (WT) were injected orthotopically with 1x10^5 LSL-KRASG12D/WT; LSL-Trp53R172H/WT; p48Cre/WT (KPC) 4662 cells into the pancreas at Day 0 and exercise was started at Day 1. Control mice remained sedentary. Mice were sacrificed at Day 21. Representative tumor images (left) and quantification of tumor

weights (right) are shown. Scale bar represents 1 cm. Each dot represents one tumor (n = 7). d. 8- week old female WT mice were injected orthotopically with 5x10^4 KPC 4662 cells into the pancreas at Day 0. At Day 12 following implantation, mice were randomized into control and exercise cohorts. Mice were sacrificed at Day 28. Schematic of experimental design (top), tumor images (bottom) and quantification of tumor weights (right) are shown. Scale bar represents 1 cm. Each dot represents one tumor (n = 9-10). ($p < 0.05$ = *, $p < 0.001$ = **, $p < 0.0001$ = ****).

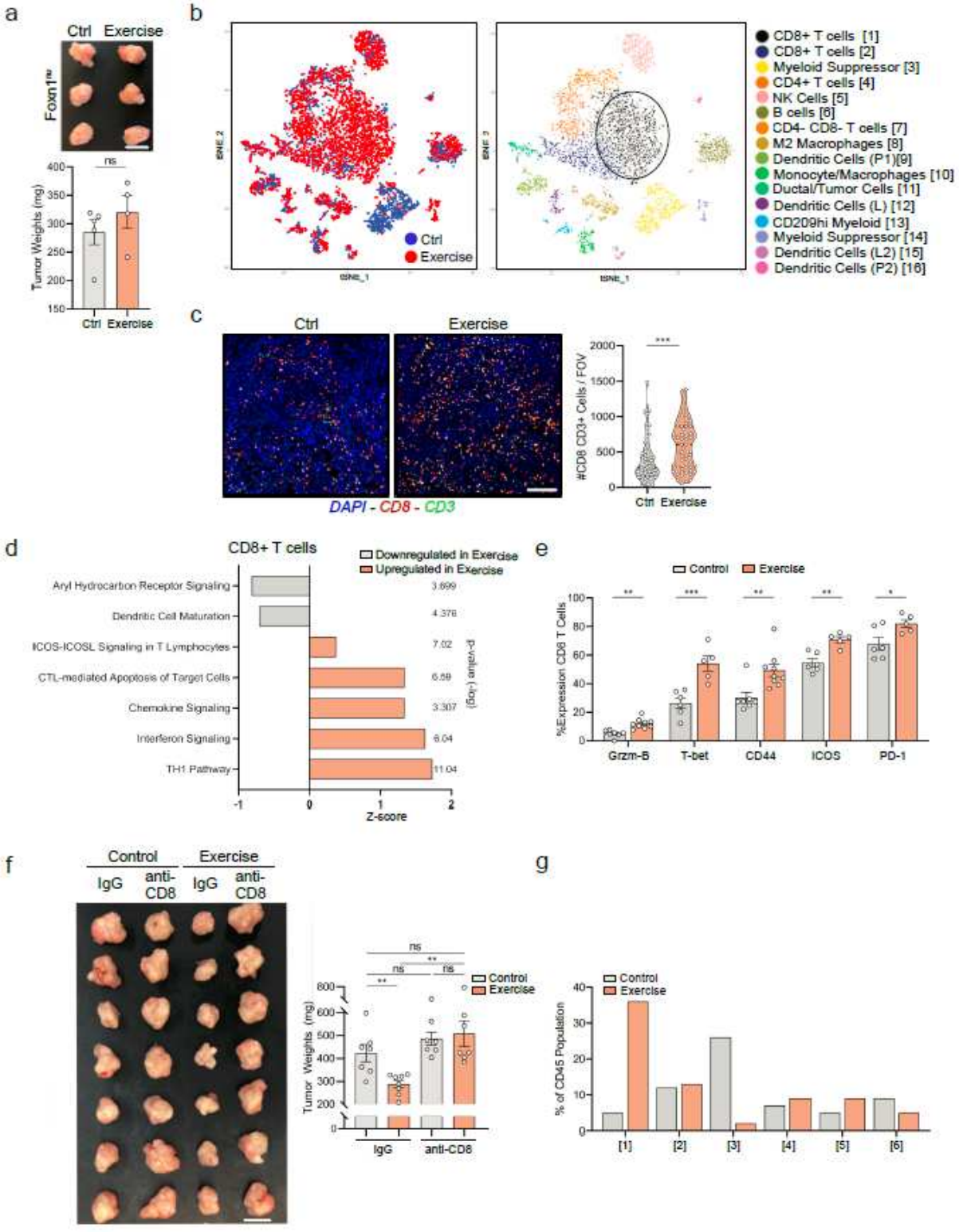

Figure 2

The tumor protective effects of aerobic exercise are dependent on CD8 T cells a. 8 week old female athymic nude NU/J mice were injected orthotopically with 1x10^5 KPC 4662 cells at Day 0 and exercise was started at Day 1. Control mice remained sedentary. Mice were sacrificed at Day 21. Representative tumor images (top) and quantification of tumor weights (below) are shown. Scale bar represents 1 cm. Each dot represents one tumor (n =4-5). b-g. 8- week old female C57BL/6J wild type mice (WT) were injected orthotopically with 1x10^5 KPC 4662 cells into the pancreas at Day 0 and exercise was started at Day 1. Control mice remained sedentary. Mice were sacrificed at Day 21 and tumors analyzed as follows. b. Single cell RNASeq (scRNAseq) was performed on live leukocytes (PI-, CD45+) isolated by FACS. The distribution of cellular clusters was determined using the tSNE algorithm: control (blue) and exercise (red) leukocytes were identified (left), phenotypic clusters were identified by distinct colors (middle) and labeled (right) (n = 3 tumors pooled in each group). c. Tumor sections were stained by multiplex immunofluorescence for CD8 (red), CD3 (green), and DAPI (blue). The number of CD8+ CD3+ (yellow) cells were quantified in ImageJ. Each dot represents quantification in one field of view (13-16 FOV analyzed; n=4). Scale bar represents 75 μm. d. Upstream canonical pathway perturbations were derived using ingenuity pathway analysis. Pathways up-regulated (orange) or down-regulated (grey) in exercise were identified in the CD8+ T cell, Cluster 1. e. Single cell suspensions derived from tumors were stained with antibodies against CD45, CD3, CD4, CD8, Granzyme-B, T-bet, CD44, ICOS, and PD-1 and analyzed by flow cytometry. Each dot represents one tumor (n=6). f. Control and exercise mice were treated 3x/week with isotype or 200 μg of α-CD8 blocking antibody starting on Day 1. Tumor images (left) and quantification of tumor weights (right) are shown. Scale bar represents 1 cm. Each dot represents one tumor (n=7). g. Quantification of the relative proportion of the six most prominent immune populations in control and exercise tumors from scRNAseq. ($p > 0.05$ = ns, $p < 0.05$ = *, $p < 0.01$ = **, $p < 0.001$ = ***).

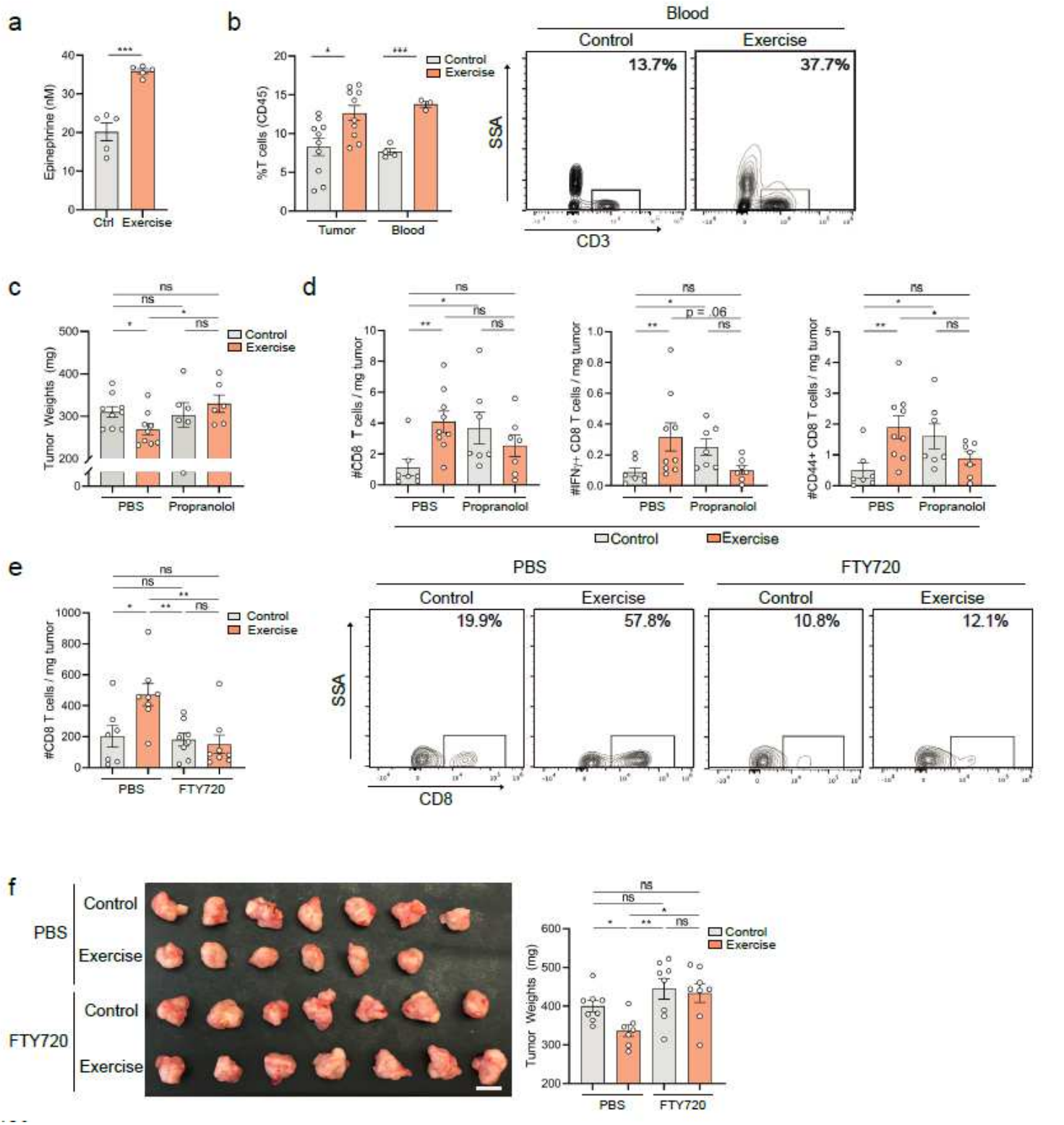

Figure 3

Exercise-induced increase in intra-tumoral CD8 T cells is β-adrenergic and S1P gradient dependent. a. 8 week-old female WT mice were exercised for 30 minutes at 15cm/sec and were sacrificed 20 minutes after completion of exercise. 200 µl of whole blood was collected, sera were isolated using centrifugation, and samples were subjected to ELISA for detection of Epinephrine levels. Each dot represents one mouse (n = 5). b-f. 8-week old female C57BL/6J wild type mice (WT) were injected orthotopically with 1x10^5

KPC 4662 cells into the pancreas at Day 0 and exercise was started at Day 1. Control mice remained sedentary. b. Mice were sacrificed at Day 21, thirty minutes after completion of exercise, and tumors and whole blood were harvested, digested, and assessed for relative numbers of CD3+ T cells. Each dot represents one mouse (n =3-4 each for blood, n= 10 for tumors). Representative contour plots are shown for CD3+ cells as a percentage of CD45+ cells in whole blood. c-d. Mice were provided with either normal drinking water or .5g/L propranolol drinking water ad libitum starting on Day 1. Mice were sacrificed on Day 21 and tumor weights were quantified (c), and single cell suspensions derived from tumors were stained with antibodies against CD45, CD3, CD8, IFNg, and CD44 and analyzed by flow cytometry (d). Each dot represents one tumor (n= 6-9). e-f. Mice were treated daily either with PBS or 200 µl of fingolimod (FTY720) starting on Day 1. Mice were sacrificed at Day 21. Single cell suspensions derived from tumors were stained with antibodies against CD45, TCRB, CD4, and CD8, and analyzed by flow cytometry. Each dot represents one tumor. Representative flow cytometry plots are shown for CD8+ cells as fraction of CD4– CD3+ cells (e). Tumor images (left) and quantification of tumor weights (right) are shown (f). Scale bar represents 1 cm. Each dot represents one tumor (n =7). ($p > 0.05$ = ns, $p < 0.05$ = *, $p < 0.01$ = **, $p < 0.001$ = ***).

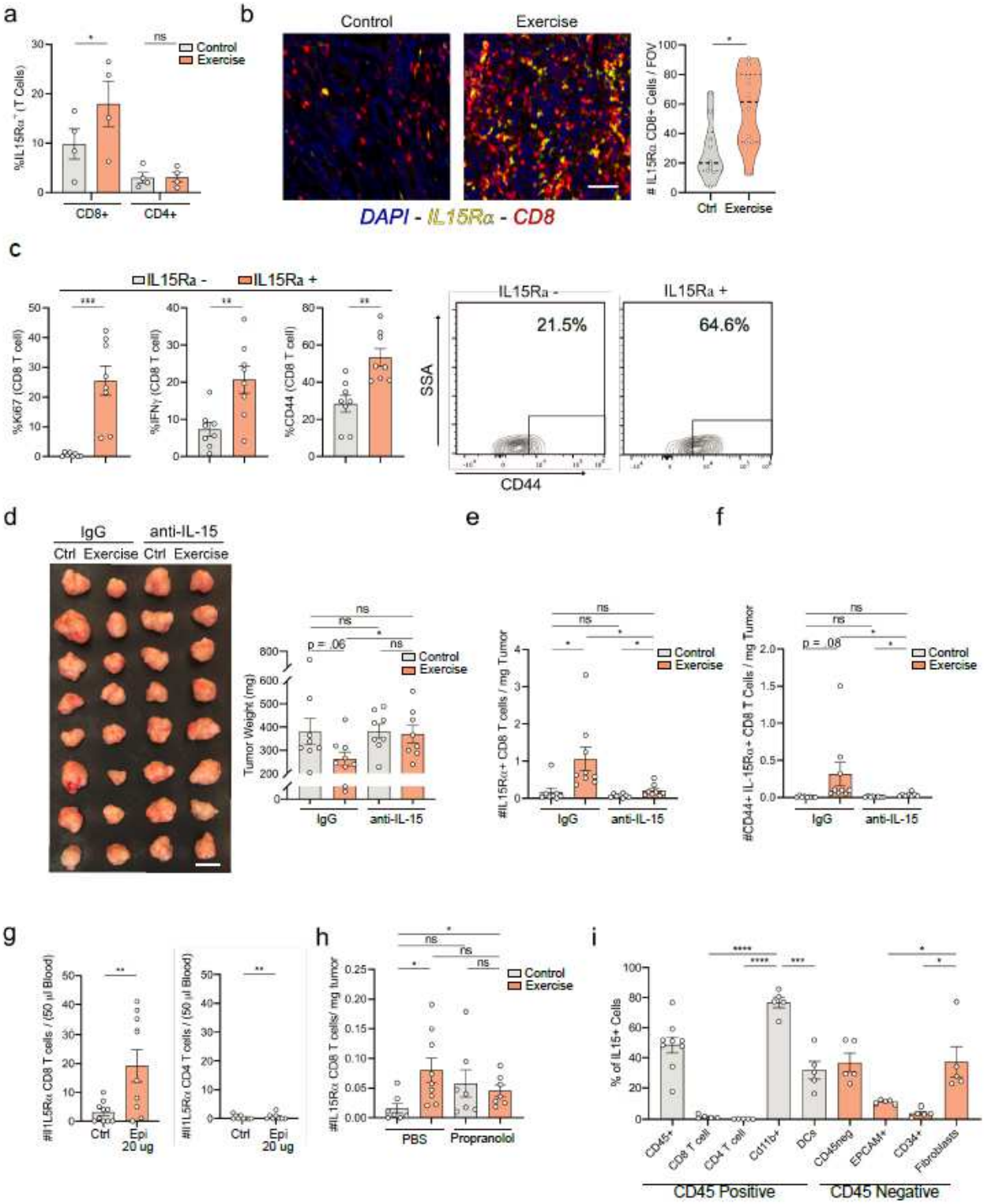

Figure 4

IL-15/IL15Rα axis is required for exercise-mediated tumor protection a-f. 8-week old female C57BL/6J wild type mice (WT) were injected orthotopically with 1x10^5 KPC 4662 cells into the pancreas at Day 0 and exercise was started at Day 1. Control mice remained sedentary. Mice were sacrificed at Day 21 and tumors analyzed as follows. a. Single cell suspensions derived from tumors were stained with antibodies against CD45, CD3, CD4, CD8, and IL-15Rα and analyzed by flow cytometry. Each dot represents one

tumor (n=4). b. Tumor sections were stained by multiplex immunofluorescence for CD8 (red), IL-15Rα (yellow), and DAPI (blue). The number of CD8+ IL-15Rα+ (orange) cells were quantified in ImageJ. Each dot represents quantification per field of view (3-4 FOV analyzed; n=3). Scale bar represents 40 μm. c. Single cell suspensions derived from tumors were stained with antibodies against CD8, Ki67, IFNg, CD44 and IL-15Rα and analyzed by flow cytometry. Each dot represents one tumor (n=8). Representative flow cytometry plots are shown for CD44. d-f. Mice were treated 3x/week with isotype or 200 μg of α-IL15 neutralizing antibody starting on Day 1 post-op. Tumor images (left) and quantification of tumor weights (right) are shown. Scale bar represents 1 cm (d). Single cell suspensions derived from tumors were stained and analyzed by flow cytometry for number of IL- 15Rα+ CD8+ T cells (e) and CD44+ IL-15Rα+ CD8+ T cells (f). Each dot represents one tumor (n=8-9). g. 9-week-old female WT mice were injected i.p. with PBS or 20 μg of Epinephrine. Thirty minutes post-treatment 100 μl of whole blood was isolated and assessed by flow cytometry for number of IL-15Rα+ CD8+ T cells (left) or IL-15Rα+ CD4+ T cells (right). Each dot represents one mouse (n =9-10). h. 8-week old female C57BL/6J wild type mice (WT) were injected orthotopically with 1x10^5 KPC 4662 cells into the pancreas at Day 0 and exercise was started at Day 1. Control mice remained sedentary. Mice were provided either normal drinking water or .5g/L propranolol drinking water ad libitum starting on Day 1. Mice were sacrificed at Day 21. Single cell suspensions derived from tumors were assessed by flow cytometry for number of IL- 15Rα+ CD8+ T cells. Each dot represents one tumor (n= 6-9). i. 8-week old female C57BL/6J wild type mice (WT) were injected orthotopically with 1x10^5 KPC 4662 cells into the pancreas at Day 0. All mice remained sedentary. Single cell suspensions derived from tumors were stained with antibodies against CD45, CD3, CD8 T cells (CD8+ CD3+), CD4 T cells (CD4+ CD3+), CD11b, DCs (CD11c+ MHCII hi), EPCAM, CD34, Fibroblasts (CD140a+ CD34- EPCAM CD45-) and analyzed by flow cytometry for the expression of IL-15. Each dot represents one tumor (n=5-9). ($p > 0.05$ = ns, $p < 0.05$ = *, $p < 0.01$ = **, $p < 0.001$ = ***, $p < 0.0001$ = ****).

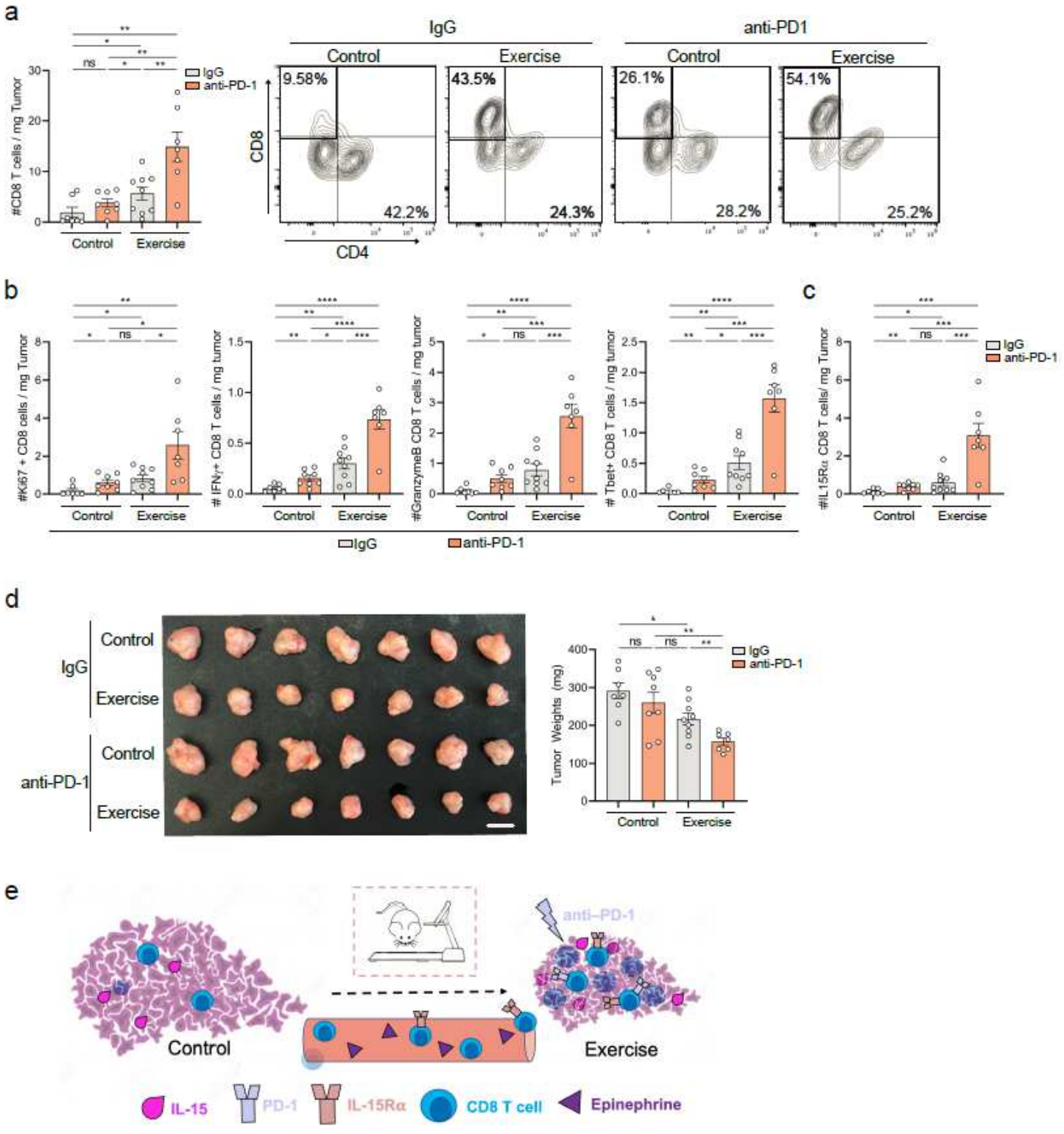

Figure 5

Aerobic Exercises Sensitizes Pancreatic Cancer to anti-PD1 Immunotherapy a-d. 8-week old female C57BL/6J wild type mice (WT) were injected orthotopically with 1x10^5 KPC 4662 cells into the pancreas at Day 0 and exercise was started at Day 1. Control mice remained sedentary. Mice were treated 3x/week with isotype or 200 µg of α-PD-1 blocking antibody starting on Day 3. Mice were sacrificed at Day 21. Single cell suspensions derived from tumors were assessed by flow cytometry for CD3, CD4, and CD8 (a),

for Ki67, Granzyme-B, T bet, and IFNg expression on CD8 T cells (b) and number of IL-15Rα+ CD8+ T cells (c). Tumor images (left) and quantification of tumor weights (right) are shown (d). Scale bar represents 1 cm. Each dot represents one tumor (n=7-8). e. Schematic depicting proposed mechanism for the impact of aerobic exercise on CD8 T cell mobilization, pancreatic tumor growth and anti-tumor immunity. ($p > 0.05$ = ns, $p < 0.05$ = *, $p < 0.01$ = **, $p < 0.001$ = ***, $p < 0.0001$ = ****).